# Synthesis, CoMFA Analysis, and Receptor Docking of 3,5-Diacyl-2,4-Dialkylpyridine Derivatives as Selective $A_3$ Adenosine Receptor Antagonists

An-Hu Li, Stefano Moro, Nancy Forsyth, Neli Melman, Xiao-duo Ji, and Kenneth A. Jacobson*

*Molecular Recognition Section, Laboratory of Bioorganic Chemistry, National Institute of Diabetes, Digestive and Kidney Diseases, National Institutes of Health, Bethesda, Maryland 20892-0810*

*Received September 29, 1998*

3,5-Diacyl-2,4-dialkyl-6-phenylpyridine derivatives have been found to be selective antagonists at both human and rat $A_3$ adenosine receptors (Li et al. *J. Med. Chem.* **1998**, *41*, 3186−3201). In the present study, ring-constrained, fluoro, hydroxy, and other derivatives in this series have been synthesized and tested for affinity at adenosine receptors in radioligand binding assays. $K_i$ values at recombinant human and rat $A_3$ adenosine receptors were determined using [$^{125}$I]AB-MECA ($N^6$-(4-amino-3-iodobenzyl)-5′-*N*-methylcarbamoyladenosine). Selectivity for $A_3$ adenosine receptors was determined vs radioligand binding at rat brain $A_1$ and $A_{2A}$ receptors, and structure−activity relationships at various positions of the pyridine ring (the 3- and 5-acyl substituents and the 2- and 4-alkyl substituents) were probed. At the 5-position inclusion of a $\beta$-fluoroethyl (**7**) or a $\gamma$-fluoropropyl ester (**26**) was favorable for human $A_3$ receptor affinity, resulting in $K_i$ values of 4.2 and 9.7 nM, respectively, while the pentafluoropropyl analogue was clearly less potent at human $A_3$ receptors. At the 2-, 3-, and 4-positions, fluoro or hydroxy substitution failed to enhance potency and selectivity at human $A_3$ receptors. Several analogues were nearly equipotent at rat and human $A_3$ receptors. To further define the pharmacophore conformationally, a lactam, a lactone, and thiolactones were tested in adenosine receptor binding. The most potent analogue in this group was compound **34**, in which a thiolactone was formed between 3- and 4-positions and which had a $K_i$ value of 248 nM at human $A_3$ receptors. Using affinity data and a general pharmacophore model for $A_3$ adenosine receptor antagonists recently proposed, we applied comparative molecular field analysis (CoMFA) to obtain a three-dimensional quantitative structure−activity relationship for pyridine derivatives, having good predictability ($r^2_{pred} = 0.873$) for compounds in the test set. A rhodopsin-based model of the human $A_3$ receptor was built, and the pyridine reference ligand 2,3,4,5-tetraethyl-6-phenylpyridine-3-thiocarboxylate-5-carboxylate (MRS 1476) was docked in the putative ligand binding site. Interactions between receptor transmembrane domains and the steric and the electrostatic contour plots obtained from the CoMFA analysis were analyzed.

## Introduction

Selective antagonists belonging to a variety of chemical classes have been reported for adenosine $A_3$ receptors.[1] Such antagonists are sought as potential antiinflammatory, antiasthmatic, or antiischemic agents.[2−5] The ligand requirements of the $A_3$ receptor are unique within the class of adenosine receptors,[6] and there are also pronounced species differences in antagonist affinity.[7−9] Xanthines, such as caffeine and theophylline, which have provided versatile leads for antagonists at the other adenosine receptor subtypes, are much less potent at the $A_3$ receptor; thus, it has been necessary to use library screening to identify novel leads (Figure 1). 1,4-Dihydropyridines (e.g., MRS 1191, **1**),[10−12] triazoloquinazolines (e.g., MRS 1220, **2**),[13] flavonoids,[14] a triazolonaphthyridine (L-249313, **3**),[15] pyridines (e.g., MRS 1523, **4**),[16] and isoquinolines (e.g. VUF 8504, **5**)[17] have been reported as $A_3$ receptor selective antagonists.

In the present study, we have further explored structure−activity relationships (SARs) for the 1,3-diacylpyridines, both previously reported[16] and newly synthesized, through oxidation of the corresponding 1,4-dihydropyridines, as antagonists of high selectivity for human $A_3$ receptors. Moderate selectivity for rat $A_3$ receptors was also present. Fluoro, hydroxy, and other derivatives in this series, which otherwise have a highly hydrophobic character, have been synthesized and tested for affinity at adenosine receptors in radioligand binding assays. Sterically constrained (bicyclic) analogues were designed and prepared for purposes of conformational analysis. New pyridine derivatives with higher affinity and selectivity for $A_3$ receptors and potentially improved pharmacodynamic properties have been obtained.

A three-dimensional quantitative structure−activity relationship (3D-QSAR) for pyridines as human $A_3$ receptor antagonists was obtained by applying comparative molecular field analysis (CoMFA)[17,18] and a previously reported general pharmacophore model.[19] A model of the human $A_3$ receptor, containing the docked pyridine reference ligand 2,3,4,5-tetraethyl-6-phenylpyridine-3-thiocarboxylate-5-carboxylate (MRS 1476),[16] was built and analyzed to help interpret these results. In particular, the steric and the electrostatic contour

* Correspondence to Dr. K. A. Jacobson; Chief, Molecular Recognition Section; LBC, NIDDK, NIH; Bldg. 8A, Rm. B1A-19; Bethesda, MD 20892-0810. Tel: (301) 496-9024. Fax: (301) 480-8422. E-mail: kajacobs@helix.nih.gov.

10.1021/jm980550w 
Published on Web 02/09/1999

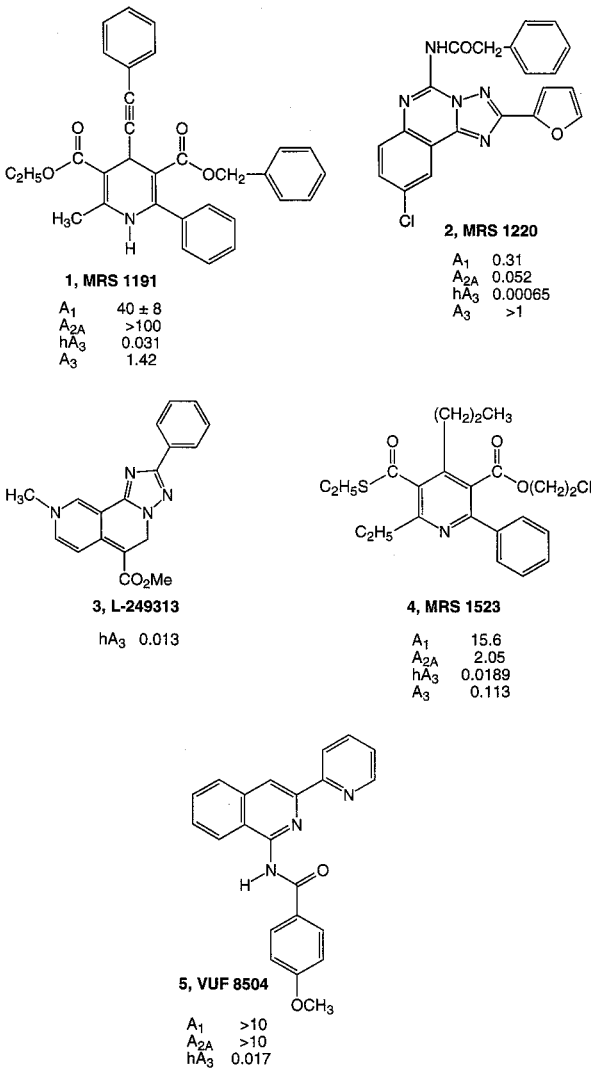


**Figure 1.** Structures of key $A_3$ adenosine receptor selective antagonists and agonists. $K_i$ values in $\mu$M were reported in refs 12−17.

plots, obtained from the CoMFA analysis of 41 pyridine derivatives, are included inside the ligand binding cavity.

## Results

**Synthesis.** Novel 3,5-diacylpyridine derivatives (**7**−**35**) were synthesized and tested for affinity in radioligand binding assays[20−22] at adenosine receptors as shown in Tables 1 and 2. As in the previous studies,[11,16] pyridine analogues were prepared from the corresponding dihydropyridines (Scheme 1) as shown.

The Hantzsch condensation, Scheme 1, which involved condensing three components, a $\beta$-enaminoester (**36**), an aldehyde (**37**), and a $\beta$-ketoester (**38**), was used for the 1,4-dihydropyridines (**39**). The corresponding pyridines were prepared through oxidation of the dihydropyridines using tetrachloroquinone (**40**). Monofluoropyridines (**7**, **14**, **19**, **21**, **24**, and **26**) were prepared by fluorinating corresponding hydroxyl-pyridines with DAST (Schemes 6, 7, and 8 in Supporting Information), and the synthesis of ring-constrained pyridine analogues is shown in Scheme 2. A lactone pyridine, **32**, thiolactone pyridines, **34** and **35**, and a lactam pyridine, **33b**, were prepared through the deprotection−intramolecular trans-

**Scheme 1.** Synthesis of Substituted 1,4-Dihydropyridines Using the Hantzsch Reaction and Oxidation to Pyridine Derivatives

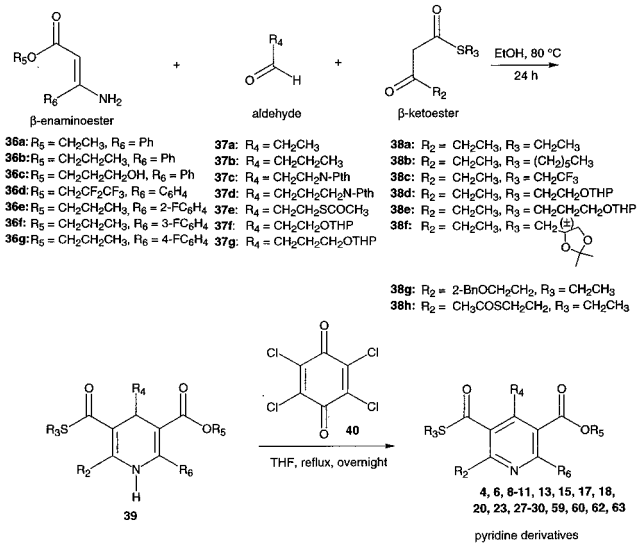


**Scheme 2.** Synthesis of Cyclic Derivatives **32**−**35**

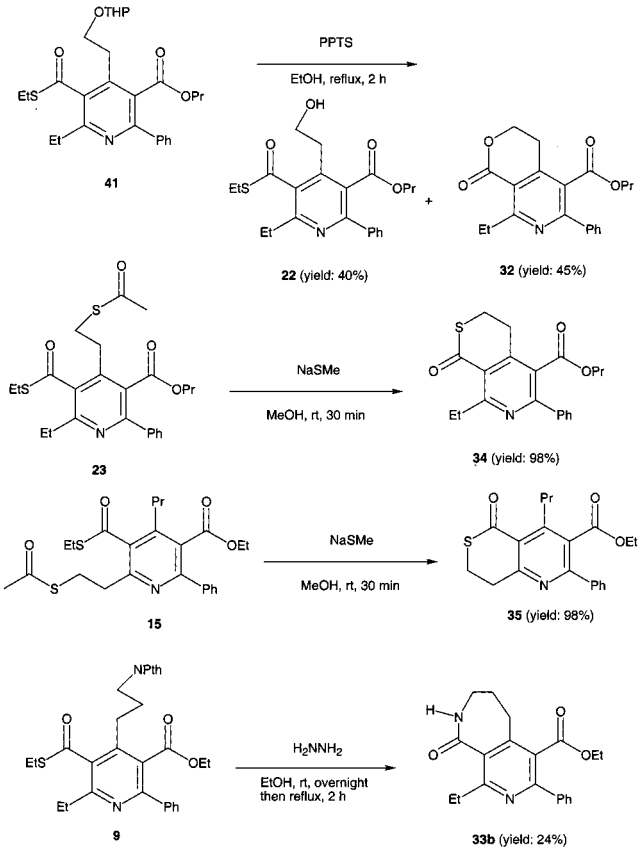


esterification of the precursor pyridine derivatives. A two-step route through acylation of Meldrum's acid (**43**),[23] followed by opening of the ring with an alcohol or thiol and decarboxylation was adopted for preparing $\beta$-ketoesters or $\beta$-ketothioesters **38** (Scheme 3), needed as precursors for the 1,4-dihydropyridines. Hydroxylated $\beta$-ketoester **46** was prepared by a transesterification reaction. Acid chlorides **42b** and **42c** were prepared as shown in Scheme 4. Thiols **50**, **51**, and **52** were prepared from selective protection of hydroxylated thiols (Scheme 4). Synthesis of protected aldehydes (**37c**−**g**)

**Table 1.** Affinities of Fluorinated and Other Pyridine Derivatives in Radioligand Binding Assays at $A_1$, $A_{2A}$, and $A_3$ Receptors

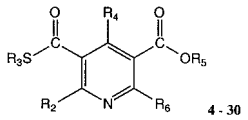


4 - 30

| | | | | | | $K_i$ (nM) or % displacement | | | |
|---|---|---|---|---|---|---|---|---|---|
| compd | $R_2$ | $R_3$ | $R_4$ | $R_5$ | $R_6$ | $rA_1$[a] | $rA_{2A}$[b] | $hA_3$[c] | $rA_1/hA_3$ |
| **4** | $CH_2CH_3$ | $CH_2CH_3$ | $CH_2CH_2CH_3$ | $CH_2CH_2CH_3$ | Ph | 15600 ± 6900 | 2050 ± 440 | 18.9 ± 4.1 | 7400 |
| **6** MRS 1476 | $CH_2CH_3$ | $CH_2CH_3$ | $CH_2CH_3$ | $CH_2CH_3$ | Ph | 41 ± 6% ($10^{-4}$) | 6130 ± 1280 | 20.0 ± 1.9 | >3000 |
| **7** | $CH_2CH_3$ | $CH_2CH_3$ | $CH_2CH_3$ | $CH_2CH_2F$ | Ph | 11500 ± 2900 | 7330 ± 1280 | 4.22 ± 0.66 | 2700 |
| **8** | $CH_2CH_3$ | $CH_2CH_3$ | $CH_2CH_2N-Pth$ | $CH_2CH_3$ | Ph | 490 ± 48 | 1140 ± 230 | 243 ± 43 | 2.0 |
| **9** | $CH_2CH_3$ | $CH_2CH_3$ | $CH_2CH_2CH_2N-Pth$ | $CH_2CH_3$ | Ph | 5240 ± 1760 | *d* ($10^{-4}$) | 28% ($10^{-6}$) | |
| **10** | $CH_2CH_3$ | $CH_2CH_3$ | $CH_2CH_3$ | $CH_2CH_2CH_3$ | Ph | 7770 ± 1830 | *d* ($10^{-5}$) | 8.29 ± 1.15 | 820 |
| **11** | $CH_2CH_3$ | $(CH_2)_5CH_3$ | $CH_2CH_3$ | $CH_2CH_2CH_3$ | 3-Cl−Ph | 113000 ± 28000 | *d* ($10^{-4}$) | 220 ± 57 | 510 |
| **12** | $CH_2CH_2OH$ | $CH_2CH_3$ | $CH_2CH_2CH_3$ | $CH_2CH_2CH_3$ | Ph | 5940 ± 930 | 29100 ± 7700 | 16% ($10^{-6}$) | |
| **13** | $CH_2CH_2O\ CH_2Ph$ | $CH_2CH_3$ | $CH_2CH_2CH_3$ | $CH_2CH_2CH_3$ | Ph | 16000 ± 1400 | 26 ± 8% ($10^{-4}$) | 109 ± 1 | 160 |
| **14** | $CH_2CH_2F$ | $CH_2CH_3$ | $CH_2CH_2CH_3$ | $CH_2CH_2CH_3$ | Ph | 19800 ± 1100 | 30800 ± 9700 | 15% ($10^{-7}$) | |
| **15** | $CH_2CH_2SCOCH_3$ | $CH_2CH_3$ | $CH_2CH_2CH_3$ | $CH_2CH_3$ | Ph | 13200 ± 2200 | 30 ± 11% ($10^{-4}$) | 193 ± 146 | 68 |
| **16** | $CH_2CH_3$ | $CH_2CH_2OH$ | $CH_2CH_2CH_3$ | $CH_2CH_2CH_3$ | Ph | 10800 ±2800 | 5590 ± 2000 | 51.1 ± 13.3 | 210 |
| **17** | $CH_2CH_3$ | $CH_2CH_2OTHP$ (rac) | $CH_2CH_2CH_3$ | $CH_2CH_2CH_3$ | Ph | 18 ± 1% ($10^{-4}$) | *d* ($10^{-4}$) | 517 ± 151 | >20 |
| **18** | $CH_2CH_3$ | $CH_2$-(2,2-dimethyl-1,3-dioxolane) (rac) | $CH_2CH_2CH_3$ | $CH_2CH_2CH_3$ | Ph | 5710 ± 1150 | *d* ($10^{-4}$) | 2640 ± 390 | 2.2 |
| **19** | $CH_2CH_3$ | $CH_2CH_2F$ | $CH_2CH_2CH_3$ | $CH_2CH_2CH_3$ | Ph | 8220 ± 3250 | 24800 ± 8000 | 55.1 ± 8.2 | 150 |
| **20** | $CH_2CH_3$ | $CH_2CF_3$ | $CH_2CH_2CH_3$ | $CH_2CH_2CH_3$ | Ph | 8290 ± 2350 | 6140 ± 1850 | 18.1 ± 2.2 | 460 |
| **21** | $CH_2CH_3$ | $CH_2CH_2CH_2F$ | $CH_2CH_2CH_3$ | $CH_2CH_2CH_3$ | Ph | 12600 ± 2800 | *d* ($10^{-4}$) | 82.8 ± 27.0 | 150 |
| **22** | $CH_2CH_3$ | $CH_2CH_3$ | $CH_2CH_2OH$ | $CH_2CH_2CH_3$ | Ph | 9040 ± 1890 | 10.3 ± 2.8 | 262 ± 57 | 35 |
| **23** | $CH_2CH_3$ | $CH_2CH_3$ | $CH_2CH_2SCOCH_3$ | $CH_2CH_2CH_3$ | Ph | 9800 ± 3490 | 28 ± 4% ($10^{-4}$) | 124 ± 29 | 79 |
| **24** | $CH_2CH_3$ | $CH_2CH_3$ | $CH_2CH_2CH_2F$ | $CH_2CH_2CH_3$ | Ph | 8090 ± 1040 | 27400 ± 8500 | 59.9 ± 17.1 | 140 |
| **25** | $CH_2CH_3$ | $CH_2CH_3$ | $CH_2CH_2CH_2OH$ | $CH_2CH_2CH_3$ | Ph | 9060 ± 2950 | 8760 ± 2490 | 169 ± 61 | 54 |
| **26** | $CH_2CH_3$ | $CH_2CH_3$ | $CH_2CH_2CH_3$ | $CH_2CH_2CH_2F$ | Ph | 6050 ± 1360 | 9670 ± 3340 | 9.67 ± 3.34 | 630 |
| **27** | $CH_2CH_3$ | $CH_2CH_3$ | $CH_2CH_2CH_3$ | $CH_2CF_2CF_3$ | Ph | 5680 ± 920 | 14000 ± 4800 | 446 ± 119 | 13 |
| **28** | $CH_2CH_3$ | $CH_2CH_3$ | $CH_2CH_2CH_3$ | $CH_2CH_2CH_3$ | 2-F−Ph | 13500 ± 1600 | 8630 ± 3550 | 23.0 ± 6.8 | 590 |
| **29** | $CH_2CH_3$ | $CH_2CH_3$ | $CH_2CH_2CH_3$ | $CH_2CH_2CH_3$ | 3-F−Ph | 8200 ± 810 | 28,100 ± 10,900 | 28.9 ± 10.8 | 280 |
| **30** | $CH_2CH_3$ | $CH_2CH_3$ | $CH_2CH_2CH_3$ | $CH_2CH_2CH_3$ | 4-F−Ph | 41000 ± 17000 | 50% ($10^{-4}$) | 31.1 ± 9.24 | 1300 |
| **31** | 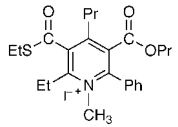 | | | | | *d* ($10^{-4}$) | *d* ($10^{-4}$) | 2020 ± 1190 | >50 |
| **32** | 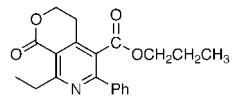 | | | | | 11200 ± 2500 | 20 ± 3% ($3 \times 10^{-5}$) | *d* ($3 \times 10^{-5}$) | |
| **33a** | 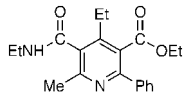 | | | | | *d* ($10^{-4}$) | *d* ($10^{-5}$) | *d* ($10^{-5}$) | |
| **33b** | 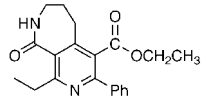 | | | | | 5790 ± 480 | *d* ($10^{-4}$) | 1990 ± 180 | 2.9 |

**Table 1** (Continued)

| | | | | |
|---|---|---|---|---|
| **34** | 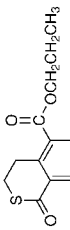 | 16500 ± 4300 | 67100 ± 23000 | 248 ± 87 | 67 |
| **35** | 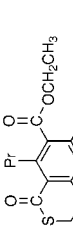 | 25100 ± 5900 | 43600 ± 13700 | 12% ($10^{-4}$) | <1 |

[a] Displacement of specific [$^3$H]*R*−PIA binding in rat brain membranes, expressed as $K_i$ ± SEM in $\mu$M ($n$ = 3−5), or as a percentage of specific binding displaced at the indicated concentration (M). [b] Displacement of specific [$^3$H]CGS 21680 binding in rat striatal membranes, expressed as $K_i$ ± SEM in $\mu$M ($n$ = 3−6), or as a percentage of specific binding displaced at the indicated concentration (M). [c] Displacement of specific [$^{125}$I]AB-MECA binding at human $A_3$ receptors expressed in HEK cells, in membranes, expressed as $K_i$ ± SEM in $\mu$M ($n$ = 3−4). [d] Displacement of ≤10% of specific binding at the indicated concentration (M); nd = not determined

**Table 2.** Affinities of 4-Phenylethynyl-6-phenyl-1,4-dihydropyridine Derivatives in Radioligand Binding Assays at Rat $A_3$ Receptors

| compd | $K_i$ (nM) r$A_3$[a] | r$A_1$/r$A_3$ | r$A_3$/h$A_3$ |
|---|---|---|---|
| **1** (MRS 1191) | 1420 ± 190 | 28 | 45 |
| **4** (MRS 1523) | 113 ± 12 | 140 | 6.0 |
| **6** (MRS 1476) | 410 ± 48 | >100 | 21 |
| **7** | 600 ± 116 | 19 | 140 |
| **10** | 183 ± 33 | 42 | 22 |
| **14** | 260 ± 24 | 76 | <1 |
| **20** | 495 ± 29 | 17 | 27 |
| **21** | 156 ± 16 | 81 | 1.9 |
| **24** | 900 ± 76 | 9.0 | 15 |
| **26** | 512 ± 39 | 12 | 53 |
| **31** | 4260 ± 680 | >23 | 2.1 |
| **34** | 2580 ± 250 | 6.4 | 10 |

[a] Displacement of specific [$^{125}$I]AB-MECA binding at rat $A_3$ receptors stably expressed in CHO cells[16,22] ($n$ = 3−5).

**Scheme 3.** Synthesis of $\beta$-Keto Esters

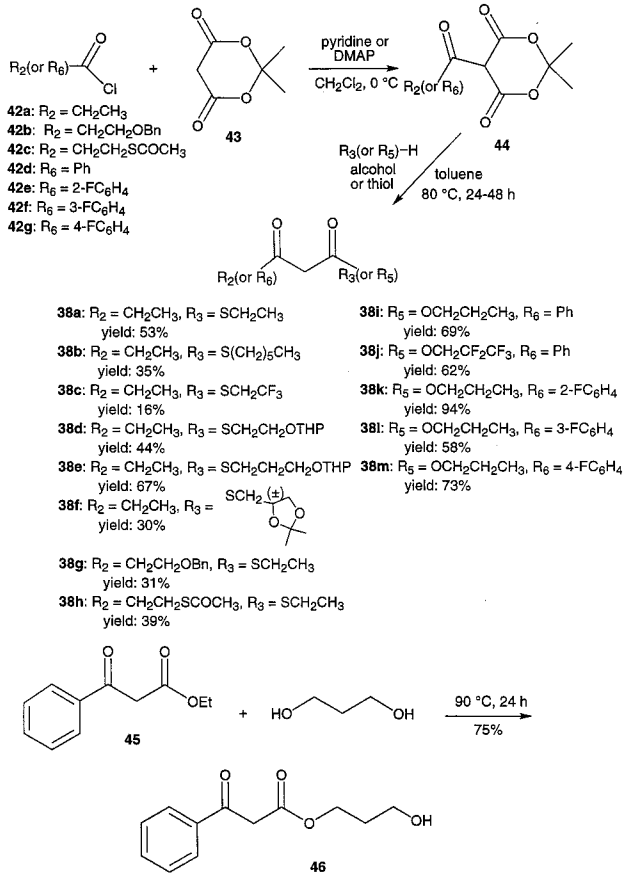


is summarized in Scheme 5. $\beta$-Enaminoesters (**36**) were made by refluxing the corresponding $\beta$-ketoesters (**38i**−**m** and **46**) and ammonium acetate in ethanol (Scheme 9 in Supporting Information). Yields and characterization of the pyridine derivatives tested as $A_3$ receptor antagonists are described in Table 3.

**Pharmacology.** The pyridine analogues previously reported as $A_3$ receptor selective antagonists, being devoid of functionality on the substituent alkyl groups, were highly hydrophobic. In an attempt to probe the electronic requirements of binding and also to introduce potentially water-solubilizing groups, we have introduced various functional groups in the analogues.

**Scheme 4.** Synthesis of Protected Intermediate Acid Chlorides and Thiols

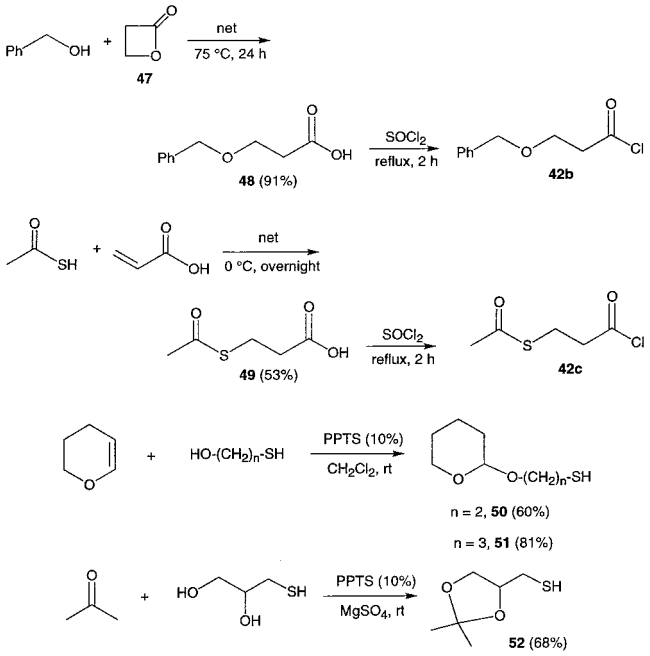


**Scheme 5.** Synthesis of Protected Intermediate Aldehydes

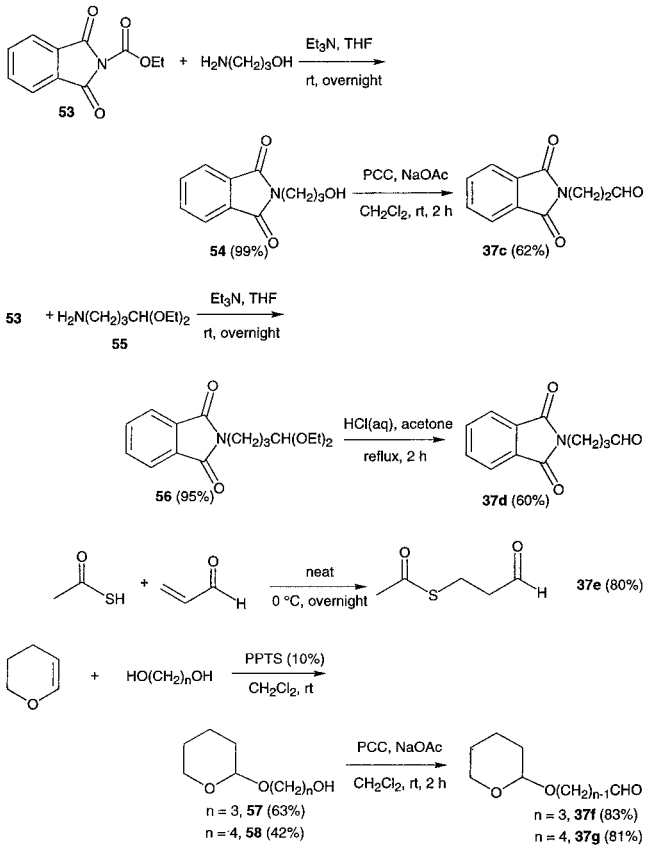


Compound **6**, a tetraethyl analogue, which was among the most potent at human $A_3$ receptors in the previous study (Table 1), was substituted with a $\beta$-fluoroethyl ester at the 5-position resulting in compound **7**, which displayed a 5-fold enhancement of affinity at human $A_3$ receptors ($K_i$ value of 4.2 nM). At the 4-position, steric bulk was introduced. A phthaloylamino analogue, **8**, was more potent than the 4-ethyl analogue, **6**, at $A_1$ receptors and less potent at $A_3$ receptors. The next higher phthaloylamino homologue, **9**, was less potent at all subtypes. The effects on receptor affinity of homologation of the alkyl groups of compound **6** were explored. Enhanced human $A_3$ affinity was observed for the 5-propyl ester, **10**, but not for the 4-propyl derivative, **4**, or for the 3-hexylthio ester-6-(3-chlorophenyl) analogue, **11**. Nevertheless, additional analogues were based on the structure of **4** rather than **10** due to its noted high affinity at rat $A_3$ receptors.[16]

The 2-ethyl group of compound **4** was modified in the form of $\beta$-hydroxyethyl, benzyloxyethyl, and acetylthioethyl substituents in compounds **12**−**15**. The hydroxy group of **12** greatly diminished affinity at human $A_3$ receptors, while a fluoro group at the same position (**14**) greatly increased affinity. The acetyl thioester of **15** was tolerated better in $A_3$ receptor binding than the bulky benzyloxy group of **13**.

Compound **16**, containing a $\beta$-hydroxyethylthio ester at the 3-position, was 3-fold less potent at $A_3$ receptors than the corresponding 3-ethylthio ester, **4**. The presence of a bulky tetrahydropyranyl group and a dioxolane group in **17** and **18**, respectively, further decreased affinity at adenosine receptors. The introduction of fluorine at the 3-thioester group in compounds **19**−**21** failed to enhance potency and selectivity at human $A_3$

**Table 3.** Yields and Analysis of Pyridine Derivatives

| no. | formula | analysis | yield (%) |
|---|---|---|---|
| **7** | $C_{21}H_{24}FNO_3S$ | HRMS[e] | 50 |
| **8** | $C_{29}H_{28}N_2O_5S\cdot0.25H_2O$ | C, H, N | 56 |
| **9** | $C_{30}H_{30}N_2O_5S$ | C, H, N | 72 |
| **11** | $C_{26}H_{34}ClNO_3S$ | C, H, N | 56 |
| **12** | $C_{23}H_{29}NO_4S$ | C, H, N | 57 |
| **13** | $C_{30}H_{35}NO_4S$ | C, H, N | 54 |
| **14** | $C_{23}H_{28}FNO_3S$ | C, H, N | 88 |
| **15** | $C_{24}H_{29}NO_4S_2\cdot0.55C_7H_8$ | C, H, N | 37 |
| **16** | $C_{23}H_{29}NO_4S$ | C, H, N | 52 |
| **17** | $C_{28}H_{37}NO_5S\cdot0.4H_2O$ | C, H, N | 8 |
| **18** | $C_{27}H_{35}NO_5S$ | C, H, N | 22 |
| **19** | $C_{23}H_{28}FNO_3S\cdot0.8C_7H_8$ | C, H, N | 73 |
| **20** | $C_{23}H_{26}F_3NO_3S$ | C, H, N | 16 |
| **21** | $C_{24}H_{30}FNO_3S\cdot1.1C_7H_8$ | C, H, N | 77 |
| **22** | $C_{22}H_{27}NO_4S$ | H, N, C[a] | 40 |
| **23** | $C_{24}H_{29}NO_4S_2\cdot0.1C_7H_8$ | C, H, N | 68 |
| **24** | $C_{23}H_{28}FNO_3S\cdot0.8C_7H_8$ | C, H, N | 83 |
| **25** | $C_{23}H_{29}NO_4S\cdot0.2C_7H_8$ | C, H, N | 86 |
| **26** | $C_{23}H_{28}FNO_3S$ | HRMS[c] | 41 |
| **27** | $C_{23}H_{24}F_5NO_3S$ | C, H, N | 66 |
| **28** | $C_{23}H_{28}FNO_3S$ | C, H, N | 80 |
| **29** | $C_{23}H_{28}FNO_3S\cdot0.15C_7H_8$ | C, H, N | 85 |
| **30** | $C_{23}H_{28}FNO_3S$ | HRMS[d] | 92 |
| **31** | $C_{24}H_{32}INO_3S\cdot0.73I_2$ | C, H, N | 22 |
| **32** | $C_{20}H_{21}NO_4$ | C, H, N | 45 |
| **33a** | $C_{20}H_{24}N_2O_3$ | C, H, N | 55 |
| **33b** | $C_{20}H_{22}N_2O_3\cdot2C_7H_8\cdot H_2O$ | C, H, N[b] | 24 |
| **34** | $C_{20}H_{21}NO_3S\cdot1.5H_2O$ | C, H, N | 98 |
| **35** | $C_{20}H_{21}NO_3S\cdot1.0H_2O$ | C, H, N | 98 |

[a] Elemental analysis for compound **22**, C: calcd, 65.81; found, 67.67. [b] Elemental analysis for compound **33**, N: d, 5.18; found, 4.18. [c] This compound was shown to be pure on analytic TLC (silica gel 60; 250 $\mu$m; EtOAc−petroleum ether = 10:90 (v/v)): compound **26**, $R_f$ = 0.49. EI calcd for $C_{23}H_{28}FNO_3S$ ($M^+$): 417.1774; found, 417.1780. [d] This compound was shown to be pure on analytic TLC (silica gel 60; 250 $\mu$m; EtOAc−petroleum ether = 10:90 (v/v)): compound **30**, $R_f$ = 0.62. EI calcd for $C_{12}H_{23}FNO_3$ ($M^+$ − SEt): 356.1662; found, 356.1667. [e] This compound was shown to be pure on analytic TLC (silica gel 60; 250 $\mu$m; EtOAc−petroleum ether = 10:90 (v/v)): compound **7**, EI calcd for $C_{21}H_{24}FNO_3S$ ($M^+$): 389.1461; found, 389.1423.

receptors, although the $\beta$-trifluoroethyl analogue, **20**, was comparable in affinity to **4**. Introduction of fluoro (**24**), hydroxy (**22**, **25**), or thioester (**23**) groups at the 4-position failed to enhance potency/selectivity.

At the 5-position propyl ester, a monofluoro substitution in compound **26** was favorable for $A_3$ affinity (similar to compound **4** above), while the pentafluoro analogue, **27**, was clearly less potent at $A_3$ receptors.

Fluoro substitution of the 6-phenyl group at ortho (**28**), meta (**29**), and para (**30**) positions produced only minor changes in the adenosine receptor affinity, while quaternization at the 1-position in the methyl pyridinium salt, **31**, resulted in moderate selectivity for human $A_3$ receptors, although affinity was greatly diminished.

To further define the pharmacophore conformationally, various ring-constrained analogues, **32**−**35**, were tested in adenosine receptor binding. The most potent analogue in this group was compound **34** ($K_i$ value of 248 nM at human $A_3$ receptors), in which a six-membered thiolactone was formed between the 3- and 4-positions. The homologous compound containing an ester instead of thioester, **32**, and an analogue containing a thiolactone formed between 2- and 3-substituents, **35**, were inactive at human $A_3$ receptors. A seven-membered lactam, **33b**, was 10-fold less potent than **34** in binding to human $A_3$ receptors. An acyclic amide derivative, **33a**, to which **33b** may be compared, was prepared and found to be inactive at human $A_3$ receptors.

Binding affinities at recombinant rat $A_3$ receptors indicated that compounds **10**, **14**, and **21** were ≥40-fold subtype selective (Table 2). The *N*-methyl pyridinium derivative, **31**, although weaker in binding, was moderately selective for rat $A_3$ vs $A_1$ receptors. The ratio of $K_i$ values at rat $A_3$ vs human $A_3$ receptors varied greatly, from <1 (compound **14**) to 140 (compound **7**), indicating specific interspecies differences in pyridine recognition. Compound **21** was nearly equipotent at rat and human $A_3$ receptors.

**Molecular Modeling. 1. CoMFA.** CoMFA 3D-QSAR methodology was applied to the data from $A_3$ binding assay as a means of identifying the structural features of pyridine derivatives (present study and ref 16) responsible for affinity. A CoMFA analysis of flavonoid derivatives as $A_3$ receptor antagonists has already been reported.[24]

PLS[39] was used in conjunction with cross-validation to obtain the optimal number of components to be used in the subsequent analyses. PLS analysis based on least-squares fit gave a correlation with a cross-validated $r^2_{cv}$ of 0.667, with the maximum number of components set equal to 3 (maximum number of components set equal to 2, 4, or 5 gave unreliable cross-validated $r^2_{cv} \leq 0.500$) and the cross-validation groups set equal to the number of observations.[40] The non-cross-validated PLS analysis was repeated with the optimum number of components, as determined by the cross-validated analysis, to give an $r^2_{cv}$ of 0.968. To obtain statistical confidence limits, the non-cross-validated analysis was repeated with 10 bootstrap groups, which yielded an $r^2$ of 0.931 (optimum number of components was 3), SEP = 0.185, standard deviation = 0.022, steric contribution = 0.571, and electrostatic contributions = 0.429. These parameters are provided in Table 5.

**Table 4.** Observed and Predicted Receptor Binding Affinity Values of the Compounds Forming the $A_3$ Test Set

| compd | p$K_i$, mM (obsvd) | p$K_i$, mM (pred)[a] |
|---|---|---|
| 10 | 8.08 | 7.92 |
| 24 | 7.22 | 7.45 |
| 27 | 6.35 | 6.55 |
| 32 | <4.5 | 4.35 |
| 35 | <4.0 | 3.98 |

[a] Values predicted by the CoMFA model.

**Table 5.** Statistic of the Calibration CoMFA Model

| | human $A_3$ |
|---|---|
| number of compounds | 41 |
| principal components[a] | 3 |
| $r^2_{cv}$[b] | 0.667 |
| $r^2$ | 0.968 |
| $F_{test}$[c] | 141.67 |
| $p$ value | <0.001 |
| $r^2_{bs}$[d] | 0.931 |
| steric contribution | 0.571 |
| electrostatic contribution | 0.429 |
| SEP[e] | 0.185 |
| std dev[f] | 0.022 |

[a] Minimum $s = 2.0$. [b] Standard error of prediction (cross-validated) = $(\text{PRESS}/(n - c - l))^{1/2}$, $n$ = number of rows, $c$ = number of components. [c] Ratio of $r^2$ explained to unexplained = $r^2/(l - r^2)$. [d] $r^2_{bs} = r^2$ after bootstrapping. [e] Cross-validated $r^2$ after leave-one-out procedure: $r^2_{cv} = (\text{SD} - \text{PRESS})/\text{SD}$, $\text{SD} = Y_{actual} - Y_{mean})^2$. $\text{PRESS} = \sum(Y_{predicted} - Y_{actual})$. For further explaination of these mathematical formulas, see ref 40. [f] The std dev column belongs with the bootstrapping $r^2$.

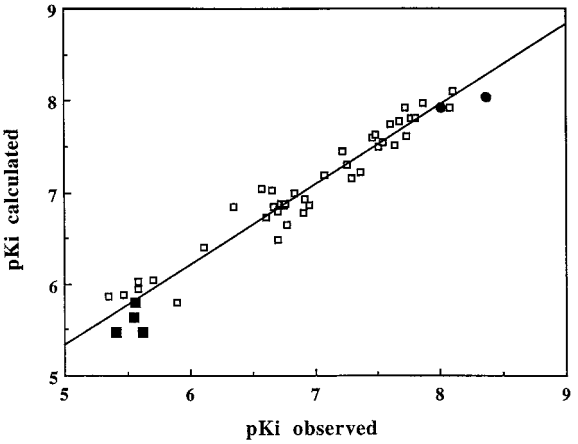


**Figure 2.** Fitted vs measured p$K_i$ values for the CoMFA analysis of human $A_3$ training set. The model was derived using three principal components yielding a cross-validated $r^2$ value of 0.667: (■) bulky substituents at the 4-position of the pyridine ring; (●) fluoro substituents at the 5-position ester group.

The CoMFA-derived QSAR of pyridine derivatives exhibited a good cross-validated correlation, indicating that it was highly predictive. Cross-validation provides information concerning the predictive ability of the QSAR data set by minimizing the occurrence of chance correlations in the QSAR model. The high bootstrapped $r^2$ value and a small standard deviation suggest a high degree of confidence in the analysis. Fitted vs measured p$K_i$ values for the CoMFA analysis of the human $A_3$ training set are shown in Figure 2.

Compounds **10, 24,** and **27** (test set) were used to evaluate the predictive power of this CoMFA model. As in the calibration step, a good predictive ability with

**Table 6.** Observed and Calculated Receptor Binding Affinity Values of the Compounds Forming the $A_3$ Training Sets

Compounds Synthesized in the Present Study

| compd | p$K_i$, $\mu$M (obsvd) | p$K_i$, $\mu$M (calcd) | compd | p$K_i$, $\mu$M (obsvd) | p$K_i$, $\mu$M (calcd) |
|---|---|---|---|---|---|
| **4** | 7.72 | 7.92 | **22** | 6.58 | 7.04 |
| **6** | 7.67 | 7.78 | **23** | 6.91 | 6.78 |
| **7** | 8.37 | 8.04 | **24** | 7.22 | 7.45 |
| **8** | 6.61 | 6.73 | **25** | 6.77 | 6.88 |
| **10** | 8.08 | 7.92 | **26** | 8.01 | 7.82 |
| **11** | 6.66 | 7.02 | **27** | 6.35 | 6.85 |
| **13** | 6.96 | 6.86 | **28** | 7.64 | 7.52 |
| **15** | 6.71 | 6.48 | **29** | 7.54 | 7.55 |
| **16** | 7.29 | 7.16 | **30** | 7.51 | 7.49 |
| **19** | 7.26 | 7.30 | **31** | 5.59 | 5.95 |
| **20** | 7.74 | 7.62 | **33b** | 5.70 | 6.05 |
| **21** | 7.08 | 7.19 | **34** | 7.60 | 7.75 |

Compounds from Ref 16

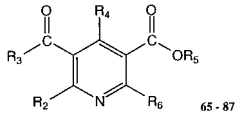


| compd | $R_2$ | $R_3$ | $R_4$ | $R_5$ | $R_6$ | p$K_i$, $\mu$M (obsvd) | p$K_i$, $\mu$M (calcd) |
|---|---|---|---|---|---|---|---|
| **65** | $CH_3$ | $OCH_2CH_3$ | $CH_3$ | $CH_2CH_3$ | Ph | 5.35 | 5.87 |
| **66** | $CH_3$ | $OCH_2CH_2CH_3$ | $CH_3$ | $CH_2CH_3$ | Ph | 6.67 | 6.85 |
| **67** | $CH_3$ | $OCH_2CH_3$ | $CH_2CH_3$ | $CH_2CH_3$ | Ph | 6.75 | 6.86 |
| **68** | $CH_3$ | $SCH_2CH_3$ | $CH_2CH_3$ | $CH_2CH_3$ | Ph | 7.37 | 7.22 |
| **69** | $CH_3$ | $SCH_2CH_2OCH_3$ | $CH_2CH_3$ | $CH_2CH_3$ | Ph | 6.78 | 6.65 |
| **70** | $CH_3$ | $SCH_2CH_3$ | $CH_2CH_2CH_3$ | $CH_2CH_3$ | Ph | 6.71 | 6.79 |
| **71** | $CH_3$ | $SCH_2CH_3$ | $CH_2CH_3$ | $CH_2Ph$ | Ph | 5.58 | 6.03 |
| **72** | $CH_3$ | $OCH_2CH_3$ | $CH(OCH_3)_2$ | $CH_2CH_3$ | Ph | 6.11 | 6.41 |
| **73** | $CH_3$ | $OCH_2CH_3$ | Ph-CH=CH− (*trans*) | $CH_2CH_3$ | Ph | 5.55 | 5.63 |
| **74** | $CH_3$ | $OCH_2CH_3$ | Ph-C≡C- | $CH_2Ph$ | Ph | 5.56 | 5.80 |
| **75** | $CH_3$ | $OCH_2CH_3$ | Ph-C≡C- | $CH_2Ph$ | cyclobutyl | 5.62 | 5.48 |
| **76** | $CH_3$ | $OCH_2CH_3$ | Ph-C≡C- | $CH_2Ph$ | cyclopentyl | 5.41 | 5.47 |
| **77** | $CH_2CH_3$ | $OCH_2CH_3$ | $CH_3$ | $CH_2CH_3$ | Ph | 6.92 | 6.92 |
| **78** | $CH_2CH_3$ | OH | $CH_2CH_3$ | $CH_2CH_3$ | Ph | 5.89 | 5.80 |
| **79** | $CH_2CH_3$ | $SCH_2CH_3$ | $CH_2CH_3$ | $CH_2CH_2OH$ | Ph | 6.73 | 6.88 |
| **80** | $CH_2CH_3$ | $SCH_2CH_3$ | $CH_2CH_3$ | $CH_2CH_3$ | 3-Cl−Ph | 7.87 | 7.97 |
| **81** | $CH_2CH_3$ | $SCH_2CH_3$ | $CH_2CH_3$ | $CH_2CH_3$ | cyclopentyl | 5.47 | 5.88 |
| **82** | $CH_2CH_3$ | $SCH_2CH_2CH_3$ | $CH_2CH_3$ | $CH_2CH_3$ | Ph | 7.80 | 7.80 |
| **83** | $CH_2CH_3$ | $SCH_2CH_2CH_3$ | $CH_2CH_3$ | $CH_2CH_2CH_3$ | 3-Cl−Ph | 8.10 | 8.10 |
| **84** | $CH_2CH_2CH_3$ | $SCH_2CH_3$ | $CH_2CH_3$ | $CH_2CH_3$ | Ph | 7.48 | 7.63 |
| **85** | $(CH_2)_2OCH_3$ | $SCH_2CH_3$ | $CH_2CH_3$ | $CH_2CH_3$ | Ph | 7.77 | 7.81 |
| **86** | $(CH_2)_3CH_3$ | $SCH_2CH_3$ | $CH_2CH_3$ | $CH_2CH_3$ | Ph | 7.46 | 7.59 |
| **87** | cyclobutyl | $SCH_2CH_3$ | $CH_2CH_3$ | $CH_2CH_3$ | Ph | 6.84 | 6.99 |

an $r^2_{pred} = 0.873$ for the compounds in the test set was obtained. Table 4 shows that the affinities of all the examined compounds were predicted within 0.25 log unit across a range of 2.00 log units (Table 6). An additional test (compounds **32** and **35**) was used to better explore the predictability of our CoMFA model. The model predicted accurately that these cyclic derivatives would be very weak antagonists at the human $A_3$ receptor.

The coefficients corresponding to each sampled field point in the resulting correlation equation were graphically contoured. Contours corresponding to the steric (green and yellow) and electrostatic (blue and red) fields are plotted together with compound **6** in Figure 3A and 3B, respectively. The polyhedra describe the regions of space where the steric and the electrostatic fields are predicted by the CoMFA model to have the greatest effect on binding affinity. The yellow and the blue polyhedra correspond to regions of the field that are predicted to decrease the $A_3$ receptor affinity, whereas the green and the red regions are predicted to increase binding affinity.

As shown in Figure 3A, a green contour around the C-2 position of pyridine moiety suggests that bulky substituents in this position (see compounds **6**, **68**, and **84**, Table 6) enhance affinity. The two ester groups at 3- and 5-positions are also surrounded by green polyhedra, suggesting that the presence of alkyl substituents increase $A_3$ receptor affinity (see compounds **10** and **21**, Table 1). Another important region of bulk tolerance is found around the meta position of the phenyl ring at the C-6 position of pyridine. In fact, a *m*-chloro derivative **80** displayed a favorable affinity. In contrast, the region of space around the C-4 position of the pyridine moiety is contained within a yellow polyhedron, suggesting that bulky substituents are not tolerated by the receptor at this position. Both styryl and phenylpropargyl derivatives (see compounds **73** and **74**, Table 6) are among the less active compounds. Substituents of high electron density were also predicted to be accepted in the side chain of both ester groups at the 3- and 5-positions (red polyhedron in Figure 3B). Accordingly, at the 5-position a $\gamma$-fluoropropyl or $\beta$-fluoroethyl ester was favorable for $A_3$ affinity, and at the 3-position fluoro substitution was tolerated (see compounds **19** and **20**, Table 1).

**2. MRS 1476 Binding Site on the Human $A_3$ Receptor.** We have recently developed a model of the

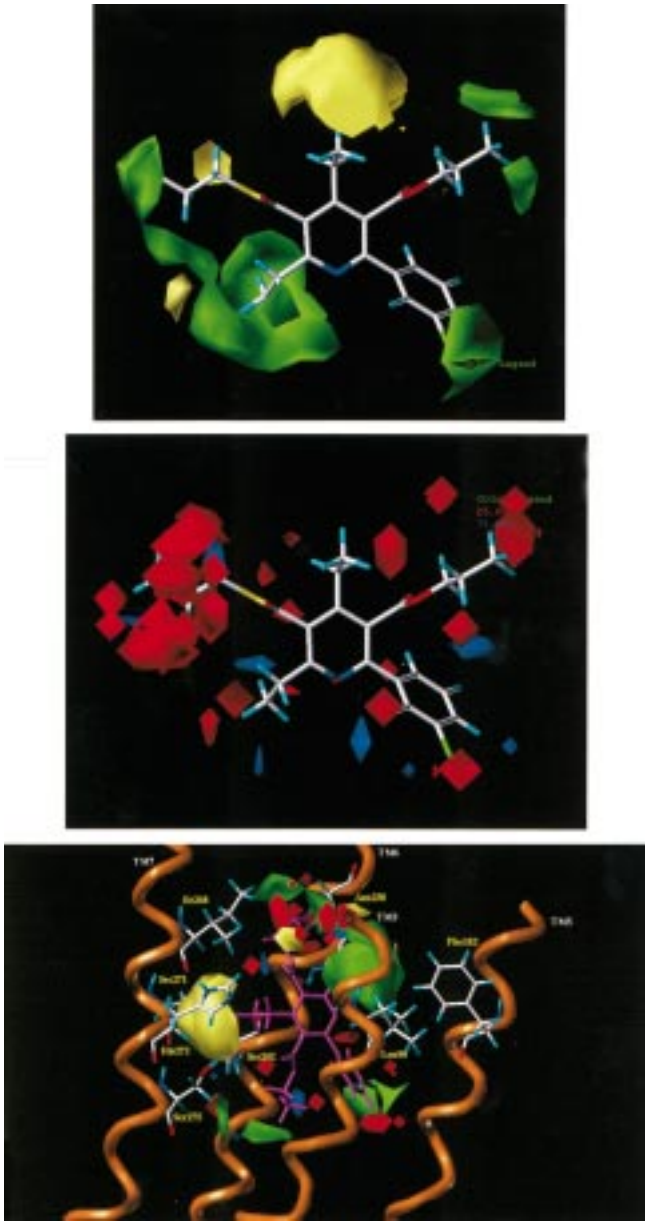

**Figure 3.** (A, top) CoMFA steric STDEV*COEFF contour plot from the analysis based on the $A_3$ receptor 3D-QSAR without cross-validation. Compound **6** shown inside the field. Favoring activity: green, bulky group (contribution level 80%); yellow, less bulky. (B, middle) CoMFA electrostatic STDEV*COEFF contour plots from the analysis based on the $A_3$ receptor 3D-QSAR without cross-validation. Compound **6** shown inside the field. Favoring activity: blue, positive charge (contribution level 70%); red, negative charge. (C, bottom) Side view of the **6**−$A_3$ complex model. The side chains of the important residues in proximity (≤5 Å) to the docked pyridine molecule are highlighted and labeleδ: Leu90 (TM3), Phe182 (TM5), Ser242 (TM6), Ser247 (TM6), Asn250 (TM6), Ser271 (TM7), His272 (TM7), Ser275 (TM7). The steric and the electrostatic contour plots, obtained from the CoMFA analysis, are included into ligand binding cavity.

human $A_3$ receptor, using rhodopsin as a template, by adapting a facile method to simulate the reorganization of the native receptor structure induced by the ligand coordination (*cross-docking* procedure).[25] Details of the model building are given in the Experimental Section. Like other G protein-coupled receptor models,[26] the length of the membrane-spanning region is about 40 Å. The interhelical distance between the pairs of adjacent helical axes is roughly 10 Å, consistent with a common interhelical contact distance.[19] The interhelical angles, measured between the principal axes of adjacent helices, range between −150 to 170° for antiparallel, and 10 to 25° for the parallel helices. This is typical of a 3−4 type helix−helix contact associated with optimal interactions between nearly parallel aligned helices.[19] After cross-docking, each helix maintained almost the same position and tilt angle found in the published rhodopsin 2D electron density map.[27,28] Moreover, in the cross-docked model, TM3, TM4, TM5, TM6, and TM7 were rotated clockwise 10°, 0°, 10°, 5°, and 10°, respectively, about their transmembrane axes with respect to the ligand-free receptor model. The energy of the cross-docked MRS 1476-receptor complex structure is about 65 kcal/mol lower with respect to the starting structure.

As previously reported, the recognition of MRS 1476 (**6**)[16,19] seems to occur in the upper region of the helical bundle. The steric and the electrostatic contour plots obtained from the CoMFA analysis without cross-validation have been included in the MRS 1476 binding site of the human $A_3$ receptor (Figure 3C). This representation emphasizes the putative microscopic interactions between ligand and receptor. The pyridine moiety of **6** is most favorably oriented perpendicular to the plane of the lipid bilayer with the carbonyl of the 5-ester group in proximity to Ser275 (TM7) and the carbonyl of the 3-ester group close to Asn250 (TM6). Two important hydrophilic interactions are hydrogen bonds between the two ester groups and these two polar amino acids. The TM7 backbone is close to the 4-position of the pyridine ring. A strong steric control around the 4-position of the pyridine structure is suggested. Two hydrophobic pockets are likely present around the 2-position, where an alkyl side chain would bind (Leu90, TM3 and Phe182, TM5), and around the 6-position where the phenyl ring would bind (Leu90, TM3 and Ile186, TM5).

## Discussion

We have identified subtle structural modifications of pyridines which lead to enhanced potency or selectivity at $A_3$ receptors. Fluoro derivatives, **7** and **26**, are the most potent pyridine derivatives in the present study. The inclusion of hydroxyl groups for potentially enhancing water solubility failed to increase $A_3$ receptor affinity.

Furthermore, the present set of analogues has allowed us to more effectively model the pyridine pharmacophore and its fit in the putative binding site of the receptor. Recently, we have published a general pharmacophore map for human $A_3$ receptor antagonists[19] derived by a combination of ab initio quantum mechanical calculations, electrostatic potential map comparison, and the steric and electrostatic alignment (SEAL) method. This general pharmacophore features the 3-position carbonyl group in the "down" position,[16] which was confirmed experimentally in the present study through the synthesis of ring-constrained analogues. The conformationally constrained lactam **33b**, in which the 3-carbonyl was "down", bound to the $A_3$ receptor with micromolar affinity, while the acyclic amide analogue **33a** was inactive. The thiolactone **34**, in which the 3-carbonyl was "down", bound to the $A_3$ receptor

with moderate affinity, while another thiolactone, **35**, in which the 3-carbonyl was "up", was inactive.

Based on the proposed pharmacophore map, we hypothesize that the receptor binding properties of different $A_3$ antagonist derivatives are due to recognition at a common region inside the receptor binding site and, consequently, a common electrostatic potential profile. To test this hypothesis computationally, we built a model of the human $A_3$ receptor, into which the pyridine MRS 1476 (**6**) was docked. Complementary interactions between the ligand and the receptor were evident, such as hydrogen bonding with Ser247 (TM7), an interaction with Asn250 (TM6), and the hydrophobic interaction with the region around Leu90 (TM3), Phe182 (TM5), and Ile186 (TM5). Perhaps the most critical interactions were between the carbonyl of the 5-ester group and Ser275 (TM7) and between the carbonyl of the 3-ester group and Asp250 (TM6). In particular, we have already reported[19] that the region of negative electrostatic potential, that in the present set of pyridines is located around the carbonyl of the ester at the 5-position, is present in all the known $A_3$ antagonist classes, such as adenines, xanthines, triazoloquinazolines, flavonoids, thiazolopyridines, and 6-phenyl-1,4-dihydropyridines. A strong steric control is suggested around the 4-position of pyridine structures, at which bulky substituents are not well tolerated, and which in our model is very close to the pyridine 4-position. In contrast, in the 1,4-dihydropyridines[10−12] bulky substituents at the 4-position enhance the $A_3$ affinity. As we have previously proposed,[19] changing the $C_4$-hybridization from $sp^3$ to $sp^2$, corresponding to the transformation of 1,4-dihydropyridine to pyridine, would change the $C_5-C_4-R_4$ angle from 68.1° to 0.2°. In this way, the 1,4-dihydropyridine 4-position substituent is positioned between TM6 and TM7. Moreover, as presented in this paper, the introduction of polar substituents, such as a fluorine atom, in the side chain of both ester groups in 3- and 5-position increases the ligand affinity.

To better analyze the steric and the electrostatic requirements of the $A_3$ receptor binding cavity, we decided to include the steric and the electrostatic contour plots obtained from the CoMFA analysis inside the MRS 1476 binding site. As shown in Figure 3C, the proposed pharmacophore model fits very well within the transmembrane binding cleft.

In conclusion, pyridine derivatives have served as structural scaffolds for enhancement of selectivity at human $A_3$ receptors and as important modeling probes for the study of the human $A_3$ receptor binding site and interspecies differences.

## Experimental Section

**Synthesis. Materials and Instrumentation.** 2-Mercaptoethanol, 3-mercapto-1-propanol, 3-mercapto-1,2-propanediol, 2,2,2-trifluoroethanethiol, hexanethiol, ethanethiol, thionyl chloride, benzyl alcohol, thiolacetic acid, $\beta$-propiolactone (**47**), acrolein, acrylic acid, 1-propanol, 1,3-propanediol, 2,2,3,3,3-pentafluoropropanol, ammonium acetate, ethyl benzoyl acetate (**45**), 3,4-dihydro-2*H*-pyran, 3-amino-1-propanol, 1,4-butanediol, 4-aminobutyraldehyde diethylacetal (**55**), *N*-carbethoxyphthalimide (**53**), tetrachloro-1,4-benzoquinone (**40**), 2,2-dimethyl-1,3-dioxane-4,6-dione (**43**), aldehydes (**37**, except for **37c**−**g**), all acid chlorides (**42**, except **42b** and **42c**, obtained by the reaction of the precursor acids with thionyl chloride), pyridinium chlorochromate (PCC), pyridinium *p*-toluenesulfonate (PPTS), diethylaminosulfur trifluoride (DAST), sodium acetate, hydrazine, and sodium thiomethoxide were purchased from Aldrich (St. Louis, MO). 5-(2-Hydroxylethyl) 2-ethyl-4-ethyl-3-(ethylsulfanylcarbonyl)-6-phenylpyridine-5-carboxylate (**59**) and MRS1523 (**4**) were prepared by our previous method.[16] All other materials were obtained from commercial sources.

Proton nuclear magnetic resonance spectroscopy was performed on a Varian GEMINI-300 spectrometer, and all spectra were obtained in $CDCl_3$. Chemical shifts ($\delta$) relative to tetramethylsilane are given. Chemical-ionization (CI) mass spectrometry was performed with a Finnigan 4600 mass spectrometer, and electron-impact (EI) mass spectrometry with a VG7070F mass spectrometer at 6 kV. Elemental analysis was performed either by Atlantic Microlab Inc. (Norcross, GA) or by Galbraith Laboratories, Inc. (Knoxville, TN).

**Two-Step Process for Preparation of Pyridine Derivatives: Hantzsch Condensation and Subsequent Oxidation (Scheme 1). Hantzsch Condensation**: Equimolar amounts (0.5−1.0 mmol) of the appropriate $\beta$-enaminoester (**36**), aldehyde (**37**), and $\beta$-ketoester (**38**) were dissolved in 2−5 mL of absolute ethanol (for preparing compound **27**, 2,2,3,3,3-pentafluoropropanol was used instead of ethanol). The mixture was sealed in a Pyrex tube and heated, with stirring, to 80 °C for 18−24 h. After the mixture cooled to room temperature, the solvent was evaporated, and the residue was purified by preparative TLC (silica 60; 1000 or 2000 mm; Analtech, Newark, DE; petroleum ether−ethyl acetate (4:1−9:1)). These 1,4-dihydropyridines (**39**) were directly used in the next step without further purification.

**Oxidation of 1,4-Dihydropyridines into Corresponding Pyridine Derivatives**. Equimolar amounts of the 1,4-dihydropyridines (**39**, ~0.2 mmol) and tetrachloro-1,4-benzoquinone (**40**) in THF (2−4 mL) were mixed and refluxed overnight. After the mixture cooled to room temperature, the solvent was removed, and the residue was purified by preparative TLC (silica 60; 1000 mm; Analtech, Newark, DE; petroleum ether−ethyl acetate (9:1−19:1)) to give the desired products.

**5-Ethyl 2,4-Diethyl-3-(ethylsulfanylcarbonyl)-6-phenylpyridine-5-carboxylate (7).** $^1$H NMR $\delta$: 1.24 (t, $J$ = 7.8 Hz, 3 H), 1.34 (t, $J$ = 7.8 Hz, 3 H), 1.41 (t, $J$ = 7.8 Hz, 3 H), 2.73 (q, $J$ = 7.8 Hz, 2 H), 2.87 (q, $J$ = 7.8 Hz, 2 H), 3.14 (q, $J$ = 7.8 Hz, 2 H), 4.23 (m, 2 H), 4.31 (t, $J$ = 4.8 Hz, 1 H), 4.39 (t, $J$ = 4.8 Hz, 1 H), 7.41−7.44 (m, 3 H), 7.59−7.61 (m, 2 H). MS (CI/$NH_3$): $m/z$ 390 ($M^+ + 1$, base). MS (EI): $m/z$ 389 ($M^+$), 360 ($M^+ - Et$), 329 ($MH^+ - EtS$, base), 300 ($M^+ - COSEt$).

**5-Ethyl 2-Ethyl-4-(2-phthalimidoethyl)-3-(ethylsulfanylcarbonyl)-6-phenylpyridine-5-carboxylate (8).** $^1$H NMR $\delta$: 1.02 (t, $J$ = 7.8 Hz, 3 H), 1.32 (t, $J$ = 7.8 Hz, 3 H), 1.46 (t, $J$ = 7.8 Hz, 3 H), 2.88 (q, $J$ = 7.8 Hz, 2 H), 3.09 (t, $J$ = 6.6 Hz, 2H), 3.22 (q, $J$ = 7.8 Hz, 2 H), 3.98 (t, $J$ = 6.9 Hz, 2 H), 4.24 (q, $J$ = 7.8 Hz, 2 H), 7.41−7.44 (m, 3 H), 7.62 (m, 2 H), 7.70−7.72 (m, 2 H), 7.82−7.85 (m, 2 H). MS (CI/$NH_3$): $m/z$ 517 ($M^+ + 1$, base).

**5-Ethyl 2-Ethyl-4-(3-phthalimidopropyl)-3-(ethylsulfanylcarbonyl)-6-phenylpyridine-5-carboxylate (9).** $^1$H NMR $\delta$: 0.90 (t, $J$ = 7.8 Hz, 3 H), 1.31 (t, $J$ = 7.8 Hz, 3 H), 1.33 (t, $J$ = 7.8 Hz, 3 H), 2.03 (m, 2 H), 2.71 (m, 2 H), 2.84 (q, $J$ = 7.8 Hz, 2 H), 2.98 (q, $J$ = 7.8 Hz, 2 H), 3.74 (t, $J$ = 6.9 Hz, 2 H), 3.98 (t, $J$ = 7.8 Hz, 2 H), 7.38−7.41 (m, 3 H), 7.54−7.57 (m, 2 H), 7.72−7.74 (m, 2 H), 7.86−7.88 (m, 2 H). MS (CI/$NH_3$): $m/z$ 546 ($M^+ + 2$).

**5-Propyl 2-Ethyl-4-ethyl-3-(hexylsulfanylcarbonyl)-6-(3-chlorophenyl)pyridine-5-carboxylate (11).** $^1$H NMR $\delta$: 0.72 (t, $J$ = 7.8 Hz, 3 H), 0.92 (t, $J$ = 6.9 Hz, 3 H), 1.23 (t, $J$ = 7.8 Hz, 3 H), 1.34 (t, $J$ = 7.8 Hz, 3 H), 1.31−1.36 (m, 4 H), 1.39−1.53 (m, 4 H), 1.71 (m, 2 H), 2.72 (q, $J$ = 7.8 Hz, 2 H), 2.86 (q, $J$ = 7.8 Hz, 2 H), 3.14 (t, $J$ = 6.9 Hz, 2 H), 4.04 (t, $J$ = 6.9 Hz, 2 H), 7.32−7.41 (m, 2 H), 7.49 (m, 1 H), 7.63 (s, 1 H). MS (CI/$NH_3$): $m/z$ 476 ($M^+$, base).

**Preparation of Pyridine 12 by Debenzylation of Compound 13.**[51] A mixture of a benzyloxy pyridine, **13** (81 mg, 0.16 mmol), boron trifluoride diethyl etherate (82 mg, 0.576

mmol), and ethanethiol (0.5 mL) was stirred at room temperature overnight. The reaction mixture was poured into water and extracted with ether (3 × 20 mL). The organic phases were combined, washed with water, dried over $MgSO_4$, and evaporated, leaving a crude material which was purified with preparative TLC (silica 60; 1000 mm; Analtech, Newark, DE; petroleum ether−ethyl acetate (4:1)) to give 38 mg of hydroxylpyridine, **12** (yield: 57%).

**5-Propyl 2-(2-Hydroxylethyl)-4-propyl-3-(ethylsulfanylcarbonyl)-6-phenylpyridine-5-carboxylate (12).** $^1$H NMR $\delta$: 0.65 (t, $J$ = 7.8 Hz, 3 H), 0.95 (t, $J$ = 7.8 Hz, 3 H), 1.40 (m, 2 H), 1.41 (t, $J$ = 7.8 Hz, 3 H), 1.62 (m, 2 H), 2.68 (m, 2 H), 3.07 (t, $J$ = 6.0 Hz, 2 H), 3.14 (q, $J$ = 7.8 Hz, 2 H), 3.99 (t, $J$ = 6.9 Hz, 2 H), 4.05 (t, $J$ = 6.0 Hz, 2 H), 7.42−7.45 (m, 3 H), 7.57−7.59 (m, 2 H). MS (CI/$NH_3$): $m/z$ 416 ($M^+$ + 1), 354 ($M^+$ − SEt, base).

**5-Propyl 2-(2-Benzyloxylethyl)-4-propyl-3-(ethylsulfanylcarbonyl)-6-phenylpyridine-5-carboxylate (13).** $^1$H NMR $\delta$: 0.66 (t, $J$ = 7.8 Hz, 3 H), 0.95 (t, $J$ = 7.8 Hz, 3 H), 1.38 (t, $J$ = 7.8 Hz, 3 H), 1.41 (m, 2 H), 1.63 (m, 2 H), 2.67 (m, 2 H), 3.13 (q, $J$ = 7.8 Hz, 2 H), 3.20 (t, $J$ = 7.8 Hz, 2 H), 3.95 (t, $J$ = 6.9 Hz, 2 H), 3.97 (q, $J$ = 7.8 Hz, 2 H), 4.54 (s, 2 H), 7.25−7.31 (m, 5 H), 7.38−7.42 (m, 3 H), 7.54−7.58 (m, 2 H). MS (CI/$NH_3$): $m/z$ 506 ($M^+$ + 1), 444 ($M^+$ − SEt).

**5-Ethyl 2-(2-Acetylthioethyl)-4-propyl-3-(ethylsulfanylcarbonyl)-6-phenylpyridine-5-carboxylate (15).** $^1$H NMR $\delta$: 0.95 (t, $J$ = 6.9 Hz, 3 H), 1.01 (t, $J$ = 6.9 Hz, 3 H), 1.41 (t, $J$ = 6.9 Hz, 3 H), 1.63 (m, 2 H), 2.32 (s, 3 H), 2.67 (m, 2 H), 3.11−3.18 (m, 4 H), 3.37 (q, $J$ = 6.6 Hz, 2 H), 4.11 (q, $J$ = 6.9 Hz, 2 H), 7.42−7.45 (m, 3 H), 7.59−7.63 (m, 2 H). MS (CI/$NH_3$): $m/z$ 460 ($M^+$ + 1, base).

**5-Propyl 2-Ethyl-4-propyl-3-(2-tetrahydropyranyloxylethylsulfanylcarbonyl)-6-phenylpyridine-5-carboxylate (17).** $^1$H NMR $\delta$: 0.66 (t, $J$ = 7.8 Hz, 3 H), 0.95 (t, $J$ = 7.8 Hz, 3 H), 1.34 (t, $J$ = 7.8 Hz, 3 H), 1.39 (m, 2 H), 1.52−1.83 (m, 8 H), 2.67 (m, 2 H), 2.87 (q, $J$ = 7.8 Hz, 2 H), 3.40 (t, $J$ = 6.0 Hz, 2 H), 3.54 (m, 1 H), 3.71 (m, 1 H), 3.92 (m, 2 H), 3.98 (t, $J$ = 6.9 Hz, 2 H), 4.70 (t, $J$ = 3.0 Hz, 1 H), 7.40−7.46 (m, 3 H), 7.59−7.62 (m, 2 H). MS (CI/$NH_3$): $m/z$ 500 ($M^+$ + 1).

**5-Propyl 2-Ethyl-4-propyl-3-((2,2-dimethyl-1,3-dioxolan-4-yl)methylsulfanylcarbonyl)-6-phenylpyridine-5-carboxylate (18).** $^1$H NMR $\delta$: 0.66 (t, $J$ = 7.8 Hz, 3 H), 0.95 (t, $J$ = 7.8 Hz, 3 H), 1.34 (t, $J$ = 7.8 Hz, 3 H), 1.38 (s, 3 H), 1.39 (m, 2 H), 1.47 (s, 3 H), 1.62 (m, 2 H), 2.66 (m, 2 H), 2.86 (q, $J$ = 7.8 Hz, 2 H), 3.38 (m, 2 H), 3.75 (dd, $J$ = 6.0, 8.7 Hz, 1 H), 3.98 (t, $J$ = 6.9 Hz, 2 H), 4.16 (dd, $J$ = 6.0, 8.7 Hz, 1 H), 4.39 (m, 1 H), 7.41−7.44 (m, 3 H), 7.59−7.62 (m, 2 H). MS (CI/$NH_3$): $m/z$ 486 ($M^+$ + 1, base).

**5-Propyl 2-Ethyl-4-propyl-3-(2,2,2-trifluoroethylsulfanylcarbonyl)-6-phenylpyridine-5-carboxylate (20).** $^1$H NMR $\delta$: 0.66 (t, $J$ = 7.8 Hz, 3 H), 0.97 (t, $J$ = 6.9 Hz, 3 H), 1.33 (t, $J$ = 7.8 Hz, 3 H), 1.41 (m, 2 H), 1.63 (m, 2 H), 2.65 (m, 2 H), 2.84 (q, $J$ = 7.8 Hz, 2 H), 3.98 (t, $J$ = 6.9 Hz, 2 H), 4.45 (q, $J$ = 7.8 Hz, 2 H), 7.41 (m, 3 H), 7.61 (m, 2 H). MS (CI/$NH_3$): $m/z$ 466 ($M^+$ − 1), 384 ($M^+$ − $SCH_2CF_3$, base).

**5-Propyl 2-Ethyl-4-(2-acetylthioethyl)-3-(ethylsulfanylcarbonyl)-6-phenylpyridine-5-carboxylate (23).** $^1$H NMR $\delta$: 0.65 (t, $J$ = 7.8 Hz, 3 H), 1.38 (m, 2 H), 1.40 (t, $J$ = 7.8 Hz, 3 H), 1.46 (t, $J$ = 7.8 Hz, 3 H), 2.34 (s, 3 H), 3.03−3.12 (m, 6 H), 3.28 (q, $J$ = 7.8 Hz, 2 H), 4.11 (t, $J$ = 6.9 Hz, 2 H), 7.46−7.57 (m, 3 H), 8.09 (m, 2 H). MS (CI/$NH_3$): $m/z$ 460 ($M^+$ + 1).

**5-(2,2,3,3,3-Pentafluoropropyl) 2-Ethyl-4-propyl-3-(ethylsulfanylcarbonyl)-6-phenylpyridine-5-carboxylate (27).** $^1$H NMR $\delta$: 0.95 (t, $J$ = 7.8 Hz, 3 H), 1.35 (t, $J$ = 7.8 Hz, 3 H), 1.42 (t, $J$ = 7.8 Hz, 3 H), 1.58−1.65 (m, 2 H), 2.65 (m, 2 H), 2.88 (q, $J$ = 7.8 Hz, 2 H), 3.15 (q, $J$ = 7.8 Hz, 2 H), 4.38 (t, $J$ = 12.6 Hz, 2 H), 7.42−7.44 (m, 3 H), 7.53−7.56 (m, 2 H). MS (CI/$NH_3$): $m/z$ 490 ($M^+$ + 1, base).

**5-Propyl 2-Ethyl-4-propyl-3-(ethylsulfanylcarbonyl)-6-(*o*-fluorophenyl)pyridine-5-carboxylate (28).** $^1$H NMR $\delta$: 0.73 (t, $J$ = 7.8 Hz, 3 H), 0.95 (t, $J$ = 7.8 Hz, 3 H), 1.32 (t, $J$ = 7.8 Hz, 3 H), 1.39 (m, 2 H), 1.42 (t, $J$ = 7.8 Hz, 3 H), 1.62 (m, 2 H), 2.73 (m, 2 H), 2.85 (q, $J$ = 7.8 Hz, 2 H), 3.14 (q, $J$ = 7.8 Hz, 2 H), 3.97 (t, $J$ = 6.9 Hz, 2 H), 7.11 (t, $J$ = 9.0 Hz, 1 H), 7.21 (t, $J$ = 6.0 Hz, 1 H), 7.38 (m, 1 H), 7.48 (m, 1 H). MS (CI/$NH_3$): $m/z$ 418 ($M^+$ + 1, base).

**5-Propyl 2-Ethyl-4-propyl-3-(ethylsulfanylcarbonyl)-6-(*m*-fluorophenyl)pyridine-5-carboxylate (29).** $^1$H NMR $\delta$: 0.71 (t, $J$ = 7.8 Hz, 3 H), 0.95 (t, $J$ = 7.8 Hz, 3 H), 1.34 (t, $J$ = 7.8 Hz, 3 H), 1.42 (t, $J$ = 7.8 Hz, 3 H), 1.47 (m, 2 H), 1.64 (m, 2 H), 2.65 (m, 2 H), 2.86 (q, $J$ = 7.8 Hz, 2 H), 3.13 (q, $J$ = 7.8 Hz, 2 H), 4.02 (t, $J$ = 6.9 Hz, 2 H), 7.10 (m, 1 H), 7.37 (m, 3 H). MS (CI/$NH_3$): $m/z$ 418 ($M^+$ + 1, base).

**5-Propyl 2-Ethyl-4-propyl-3-(ethylsulfanylcarbonyl)-6-(*p*-fluorophenyl)pyridine-5-carboxylate (30).** $^1$H NMR $\delta$: 0.71 (t, $J$ = 7.8 Hz, 3 H), 0.95 (t, $J$ = 7.8 Hz, 3 H), 1.33 (t, $J$ = 7.8 Hz, 3 H), 1.42 (t, $J$ = 7.8 Hz, 3 H), 1.44 (m, 2 H), 1.62 (m, 2 H), 2.65 (m, 2 H), 2.85 (q, $J$ = 7.8 Hz, 2 H), 3.13 (q, $J$ = 7.8 Hz, 2 H), 4.01 (t, $J$ = 6.9 Hz, 2 H), 7.09−7.15 (m, 2 H), 7.58−7.63 (m, 2 H). MS (EI): $m/z$ 416 ($M^+$ − 1), 356 ($M^+$ − SEt, base), 330 ($M^+$ − $CO_2Pr$).

**5-Propyl 2-Ethyl-4-(2-tetrahydropyranyloxylethyl)-3-(ethylsulfanylcarbonyl)-6-phenylpyridine-5-carboxylate (41).** $^1$H NMR $\delta$: 0.63 (t, $J$ = 7.8 Hz, 3 H), 1.34 (t, $J$ = 7.8 Hz, 3 H), 1.37 (m, 2 H), 1.42 (t, $J$ = 7.8 Hz, 3 H), 1.47−1.81 (m, 6 H), 2.88 (q, $J$ = 7.8 Hz, 2 H), 3.08 (t, $J$ = 7.8 Hz, 2 H), 3.14 (q, $J$ = 7.8 Hz, 2 H), 3.46 (m, 1 H), 3.63 (m, 1 H), 3.77 (m, 1 H), 3.89 (m, 1 H), 3.98 (t, $J$ = 6.9 Hz, 2 H), 4.58 (t, $J$ = 3.9 Hz, 1 H), 7.41−7.45 (m, 3 H), 7.58−7.61 (m, 2 H). MS (CI/$NH_3$): $m/z$ 486 ($M^+$ + 1, base).

**5-(3-Hydroxylpropyl) 2-Ethyl-4-propyl-3-ethylsulfanylcarbonyl-6-phenylpyridine-5-carboxylate (60).** $^1$H NMR $\delta$: 0.95 (t, $J$ = 7.8 Hz, 3 H), 1.34 (t, $J$ = 7.8 Hz, 3 H), 1.42 (t, $J$ = 7.8 Hz, 3 H), 1.61 (m, 2 H), 1.83 (m, 2 H), 2.66 (m, 2 H), 2.86 (q, $J$ = 7.8 Hz, 2 H), 3.14 (q, $J$ = 7.8 Hz, 2 H), 3.82 (t, $J$ = 6.9 Hz, 2 H), 4.10 (t, $J$ = 6.9 Hz, 2 H), 7.41−7.44 (m, 3 H), 7.57−7.60 (m, 2 H). MS (CI/$NH_3$): $m/z$ 416 ($M^+$ + 1).

**5-Propyl 2-Ethyl-4-(3-tetrahydropyranyloxylpropyl)-3-(ethylsulfanylcarbonyl)-6-phenylpyridine-5-carboxylate (62).** $^1$H NMR $\delta$: 0.67 (t, $J$ = 7.8 Hz, 3 H), 1.34 (t, $J$ = 7.8 Hz, 3 H), 1.41 (t, $J$ = 7.8 Hz, 3 H), 1.42 (m, 2 H), 1.54−1.96 (m, 8 H), 2.78 (m, 2 H), 2.87 (q, $J$ = 7.8 Hz, 2 H), 3.13 (q, $J$ = 7.8 Hz, 2 H), 3.41 (m, 1 H), 3.50 (m, 1 H), 3.73 (m, 1 H), 3.84 (m, 1 H), 3.99 (t, $J$ = 6.9 Hz, 2 H), 4.59 (t, $J$ = 3.0 Hz, 1 H), 7.40−7.43 (m, 3 H), 7.60−7.62 (m, 2 H). MS (CI/$NH_3$): $m/z$ 500 ($M^+$ + 1, base).

**5-Propyl 2-Ethyl-4-propyl-3-(3-tetrahydropyranyloxylpropylsulfanylcarbonyl)-6-phenylpyridine-5-carboxylate (63).** $^1$H NMR $\delta$: 0.66 (t, $J$ = 7.8 Hz, 3 H), 0.94 (t, $J$ = 7.8 Hz, 3 H), 1.33 (t, $J$ = 7.8 Hz, 3 H), 1.39 (m, 2 H), 1.54−1.86 (m, 8 H), 2.04 (m, 2 H), 2.66 (m, 2 H), 2.85 (q, $J$ = 7.8 Hz, 2 H), 3.24 (m, 2 H), 3.52 (m, 2 H), 3.88 (m, 2 H), 3.98 (t, $J$ = 6.9 Hz, 2 H), 4.61 (t, $J$ = 3.9 Hz, 1 H), 7.40−7.44 (m, 3 H), 7.59−7.61 (m, 2 H). MS (CI/$NH_3$): $m/z$ 514 ($M^+$ + 1, base).

**General Procedure For Preparing Monofluoro-pyridines: By Fluorinating Corresponding Hydroxyl-pyridines with DAST.** Under $N_2$, hydroxyl-pyridine (**59**, **60**, **25**, **64**, **16**, or **12**, ∼0.05 to ∼0.3 mmol) was dissolved in anhydrous $CH_2Cl_2$ (1−3 mL) and the solution was cooled to −78 °C. Two equivalents of DAST were then added by syringe. The reaction was stirred at −78 °C for 0.5 h before the temperature was allowed to rise to room temperature. The stirring was continued until the reaction was complete (by TLC). The reaction mixture was carefully hydrolyzed upon addition of two drops of water. The organic phase was separated, and the aqueous phase was extracted with ether. The organic phases were combined and dried with anhydrous $MgSO_4$. After the solvent was removed, the residue was purified by preparative TLC (silica 60; 1000 or 2000 mm; Analtech, Newark, DE; petroleum ether−ethyl acetate (4:1−19:1)) to provide pure monofluoropyridines (**7**, **14**, **19**, **21**, **24**, and **26**).

**5-(2-Fluoroethyl) 2-Ethyl-4-ethyl-3-(ethylsulfanylcarbonyl)-6-phenylpyridine-5-carboxylate (7).** $^1$H NMR $\delta$: 1.24 (t, $J$ = 7.8 Hz, 3 H), 1.34 (t, $J$ = 7.8 Hz, 3 H), 1.41 (t, $J$ = 7.8 Hz, 3 H), 2.73 (q, $J$ = 7.8 Hz, 2 H), 2.87 (q, $J$ = 7.8 Hz, 2 H), 3.14 (q, $J$ = 7.8 Hz, 2 H), 4.23 (m, 2 H), 4.31 (t, $J$ = 4.8 Hz, 1 H), 4.39 (t, $J$ = 4.8 Hz, 1 H), 7.41−7.44 (m, 3 H), 7.59−7.61

(m, 2 H). MS (CI/$NH_3$): *m/z* 390 ($M^+ + 1$, base). MS (EI): *m/z* 389($M^+$), 360 ($M^+ - Et$), 329 ($MH^+ - EtS$, base), 300 ($M^+ - EtSCO$).

**5-Propyl 2-(2-Fluoroethyl)-4-propyl-3-(ethylsulfanylcarbonyl)-6-phenylpyridine-5-carboxylate (14).** $^1$H NMR $\delta$: 0.66 (t, $J$ = 8.1 Hz, 3 H), 0.95 (t, $J$ = 8.1 Hz, 3 H), 1.40 (m, 2 H), 1.42 (t, $J$ = 8.1 Hz, 3 H), 1.62 (m, 2 H), 2.67 (t, $J$ = 7.8 Hz, 2 H), 3.15 (q, $J$ = 7.8 Hz, 2 H), 3.24 (t, $J$ = 6.9 Hz, 1 H), 3.30 (t, $J$ = 6.9 Hz, 1 H), 3.99 (t, $J$ = 6.9 Hz, 2 H), 4.83 (t, $J$ = 6.9 Hz, 1 H), 4.99 (t, $J$ = 6.9 Hz, 1 H), 7.41−7.43 (m, 3 H), 7.59 (m, 2 H). MS (CI/$NH_3$): *m/z* 418 ($M^+ + 1$, base).

**5-Propyl 2-Ethyl-4-propyl-3-(2-fluoroethylsulfanylcarbonyl)-6-phenylpyridine-5-carboxylate (19).** $^1$H NMR $\delta$: 0.66 (t, $J$ = 7.8 Hz, 3 H), 0.95 (t, $J$ = 7.8 Hz, 3 H), 1.34 (t, $J$ = 7.8 Hz, 3 H), 1.39 (m, 2 H), 1.64 (m, 2 H), 2.66 (m, 2 H), 2.85 (q, $J$ = 7.8 Hz, 2 H), 3.43 (t, $J$ = 6.0 Hz, 1 H), 3.50 (t, $J$ = 6.0 Hz, 1 H), 3.98 (t, $J$ = 6.6 Hz, 2 H), 4.59 (t, $J$ = 6.0 Hz, 1 H), 4.74 (t, $J$ = 6.0 Hz, 1 H), 7.42 (m, 3 H), 7.61 (m, 2 H). MS (CI/$NH_3$): *m/z* 418 ($M^+ + 1$, base).

**5-Propyl 2-Ethyl-4-propyl-3-(3-fluoropropylsulfanylcarbonyl)-6-phenylpyridine-5-carboxylate (21).** $^1$H NMR $\delta$: 0.66 (t, $J$ = 7.8 Hz, 3 H), 0.94 (t, $J$ = 7.8 Hz, 3 H), 1.34 (t, $J$ = 7.8 Hz, 3 H), 1.39 (m, 2 H), 1.62 (m, 2 H), 2.08−2.20 (m, 2 H), 2.65 (m, 2 H), 2.85 (q, $J$ = 7.8 Hz, 2 H), 3.26 (t, $J$ = 6.9 Hz, 2 H), 3.98 (t, $J$ = 6.9 Hz, 2 H), 4.51 (t, $J$ = 6.0 Hz, 1 H), 4.67 (t, $J$ = 6.0 Hz, 1 H), 7.40−7.44 (m, 3 H), 7.59−7.62 (m, 2 H). MS (CI/$NH_3$): *m/z* 432 ($M^+ + 1$, base).

**5-Propyl 2-Ethyl-4-(3-fluoropropyl)-3-(ethylsulfanylcarbonyl)-6-phenylpyridine-5-carboxylate (24).** $^1$H NMR $\delta$: 0.66 (t, $J$ = 7.8 Hz, 3 H), 1.34 (t, $J$ = 7.8 Hz, 3 H), 1.40 (m, 2 H), 1.41 (t, $J$ = 7.8 Hz, 3 H), 1.98−2.13 (m, 2 H), 2.82 (m, 2 H), 2.88 (q, $J$ = 7.8 Hz, 2 H), 3.14 (q, $J$ = 7.8 Hz, 2 H), 3.99 (t, $J$ = 6.9 Hz, 2 H), 4.37 (t, $J$ = 6.0 Hz, 1 H), 4.53 (t, $J$ = 6.0 Hz, 1 H), 7.41−7.43 (m, 3 H), 7.59−7.62 (m, 2 H). MS (CI/$NH_3$): *m/z* 418 ($M^+ + 1$, base).

**5-(3-Fluoropropyl) 2-Ethyl-4-propyl-3-(ethylsulfanylcarbonyl)-6-phenylpyridine-5-carboxylate (26).** $^1$H NMR $\delta$: 0.95 (t, $J$ = 7.8 Hz, 3 H), 1.36 (t, $J$ = 7.8 Hz, 3 H), 1.42 (t, $J$ = 7.8 Hz, 3 H), 1.65 (m, 2 H), 1.73 (m, 2 H), 2.66 (m, 2 H), 2.87 (q, $J$ = 7.8 Hz, 2 H), 3.13 (q, $J$ = 7.8 Hz, 2 H), 3.95 (t, $J$ = 6.0 Hz, 1 H), 4.11 (t, $J$ = 6.0 Hz, 1 H), 4.14 (t, $J$ = 6.0 Hz, 2 H), 7.42 (m, 3 H), 7.58 (m, 2 H). MS (CI/$NH_3$): *m/z* 418 ($M^+ + 1$, base). HRMS: calcd for $C_{23}H_{28}FNO_3S$, 417.1774; found, 417.1780.

**General Procedure For Deprotecting THP-Protected Pyridines**.[43] A mixture of THP-protected pyridine (**17**, **41**, **62**, or **63**, ~0.1 to ~0.4 mmol) and a catalytic amount of PPTS (10%) was stirred and refluxed in absolute ethanol (5−10 mL) until the reaction was complete (by TLC). After the mixture cooled to room temperature, the solvent was removed, and the residue was chromatographed on preparative TLC (silica 60; 1000 or 2000 mm; Analtech, Newark, DE; petroleum ether−ethyl acetate (4:1−9:1)) to give the hydroxyl-pyridines (**16**, **25**, or **64**). However, when the similar condition was applied to THP-pyridine **41**, besides the expected product **22**, the lactone compound **32** was also obtained through an intramolecular transesterification (Scheme 2).

**5-Propyl 2-Ethyl-4-propyl-3-(2-hydroxylethylsulfanylcarbonyl)-6-phenylpyridine-5-carboxylate (16).** $^1$H NMR $\delta$: 0.66 (t, $J$ = 7.8 Hz, 3 H), 0.95 (t, $J$ = 7.8 Hz, 3 H), 1.34 (t, $J$ = 7.8 Hz, 3 H), 1.39 (m, 2 H), 1.62 (m, 2 H), 2.68 (m, 2 H), 2.86 (q, $J$ = 7.8 Hz, 2 H), 3.53 (t, $J$ = 6.0 Hz, 2 H), 3.92 (t, $J$ = 6.0 Hz, 2 H), 3.98 (t, $J$ = 6.0 Hz, 2 H), 7.41 (m, 3 H), 7.60 (m, 2 H). MS (CI/$NH_3$): *m/z* 416 ($M^+ + 1$, base).

**5-Propyl 2-Ethyl-4-(2-hydroxylethyl)-3-(ethylsulfanylcarbonyl)-6-phenylpyridine-5-carboxylate (22).** $^1$H NMR $\delta$: 0.59 (t, $J$ = 7.8 Hz, 3 H), 1.31 (m, 2 H), 1.35 (t, $J$ = 7.8 Hz, 3 H), 1.41 (t, $J$ = 7.8 Hz, 3 H), 2.90 (q, $J$ = 7.8 Hz, 2 H), 3.00 (t, $J$ = 6.9 Hz, 2 H), 3.15 (q, $J$ = 7.8 Hz, 2 H), 3.88 (t, $J$ = 6.9 Hz, 2 H), 3.95 (t, $J$ = 6.9 Hz, 2 H), 7.41−7.46 (m, 3 H), 7.58−7.60 (m, 2 H). MS (CI/$NH_3$): *m/z* 340 ($M^+ - SEt$).

**5-Propyl 2-Ethyl-4-(3-hydroxylpropyl)-3-(ethylsulfanylcarbonyl)-6-phenylpyridine-5-carboxylate (25).** $^1$H NMR $\delta$: 0.66 (t, $J$ = 7.8 Hz, 3 H), 0.95 (t, $J$ = 7.8 Hz, 3 H), 1.34 (t, $J$ = 7.8 Hz, 3 H), 1.38 (m, 2 H), 1.63 (m, 2 H), 2.67 (t, $J$ = 6.9 Hz, 2 H), 2.87 (t, $J$ = 6.9 Hz, 2 H), 3.26 (t, $J$ = 6.9 Hz, 2 H), 3.98 (t, $J$ = 6.9 Hz, 2 H), 4.52 (t, $J$ = 6.9 Hz, 2 H), 7.42 (m, 3 H), 7.59−7.62 (m, 2 H). MS (EI): *m/z* 434 ($MH^+ + NH_4$), 387 ($MH^+ - Et$), 372 ($M^+ - Pr$), 354 ($M^+ - SEt$).

**5-Propyl 2-Ethyl-4-propyl-3-(3-hydroxylpropylsulfanylcarbonyl)-6-phenylpyridine-5-carboxylate (64).** $^1$H NMR $\delta$: 0.62 (t, $J$ = 7.8 Hz, 3 H), 1.03 (t, $J$ = 7.8 Hz, 3 H), 1.30 (m, 2 H), 1.34 (t, $J$ = 7.8 Hz, 3 H), 1.35 (m, 2 H), 1.90 (m, 2 H), 2.82 (m, 2 H), 2.87 (q, $J$ = 7.8 Hz, 2 H), 3.06 (q, $J$ = 7.8 Hz, 2 H), 3.68 (t, $J$ = 6.0 Hz, 2 H), 3.93 (t, $J$ = 6.9 Hz, 2 H), 7.37−7.45 (m, 3 H), 7.66−7.69 (m, 2 H). MS (CI/$NH_3$): *m/z* 382 ($M^+ - OEt$), 354 ($M^+ - CO_2Pr$), 324 ($M^+ - COSEt$).

**Preparation of Pyridinium Salt 31 by Quaternary Amination of Compound 4 with Iodomethane**. A mixture of **4** (MRS 1523, 40 mg, 0.1 mmol) and iodomethane (71 mg, 0.5 mmol) in 4 mL of anhydrous methanol was sealed in a Pyrex tube and heated at 80 °C for 2 days. After the mixture cooled to room temperature, the solvent and excess MeI were removed under reduced pressure, leaving a deep red tar. The tar was washed with hexanes many times to remove the unreacted MRS 1523, and 12 mg of the desired product (**31**) was afforded (yield: 22%).

**1-Methyl-2-ethyl-4-propyl-3-(ethylsulfanylcarbonyl)-5-propyloxylcarbonyl-6-phenylpyridinium Iodide (31).** $^1$H NMR $\delta$: 0.67 (t, $J$ = 7.8 Hz, 3 H), 1.04 (t, $J$ = 7.8 Hz, 3 H), 1.40 (m, 2 H), 1.48 (t, $J$ = 7.8 Hz, 3 H), 1.55 (t, $J$ = 7.8 Hz, 3 H), 1.74 (m, 2 H), 2.17 (s, 3 H), 2.87 (t, $J$ = 7.8 Hz, 2 H), 3.27 (q, $J$ = 7.8 Hz, 2 H), 3.42 (q, $J$ = 7.8 Hz, 2 H), 4.05 (t, $J$ = 7.8 Hz, 2 H), 7.62−7.74 (m, 5 H). MS (CI/$NH_3$): *m/z* 558 ($M^+ + NH_4$), 525 ($M^+ - 1 - Me$), 414 ($M^+ - I$), 369 ($M^+ - 1 - I - Me\text{-}Et$).

**Lactone (32).** $^1$H NMR $\delta$: 0.64 (t, $J$ = 7.8 Hz, 3 H), 1.37 (t, $J$ = 7.8 Hz, 3 H), 1.38 (m, 2 H), 3.12 (t, $J$ = 6.0 Hz, 2 H), 3.35 (q, $J$ = 7.8 Hz, 2 H), 4.03 (t, $J$ = 6.9 Hz, 2 H), 4.49 (t, $J$ = 6.0 Hz, 2 H), 7.45−7.47 (m, 3 H), 7.65−7.67 (m, 2 H). MS (CI/$NH_3$): *m/z* 340 ($M^+ + 1$).

**5-Ethyl 2-Methyl-4-ethyl-3-(*N*-ethylaminocarbonyl)-6-phenylpyridine-5-carboxylate (33a).** *N*-Ethyl acetoacetamide[12] (129 mg, 1.0 mmol), propionaldehyde (116 mg, 2.0 mmol), and ethyl 3-amino-3-phenyl-2-propenoate (191 mg, 1.0 mmol) were dissolved in 2 mL of absolute ethanol. The mixture was sealed in a Pyrex tube and heated, with stirring, to 90 °C overnight. After the mixture cooled to room temperature, the solvent was evaporated, and the residue was purified by preparative TLC (silica 60; 1000 mm; Analtech, Newark, DE; petroleum ether−ethyl acetate (2:1)) to give 167 mg of dihydropyridine. To a solution of this dihydropyridine in 4 mL THF was added tetrachloro-1,4-benzoquinone (40, 120 mg), and the mixture was refluxed overnight. After the mixture cooled to room temperature, the solvent was removed, and the residue was purified by preparative TLC (silica 60; 1000 mm; Analtech, Newark, DE; petroleum ether−ethyl acetate (4:1)) to give 91 mg (yield: 55%) of compound 33a. $^1$H NMR $\delta$: 0.97 (t, $J$ = 7.8 Hz, 3 H), 1.24 (t, $J$ = 7.8 Hz, 3 H), 1.27 (t, $J$ = 7.8 Hz, 3 H), 2.60 (s, 3 H), 2.72 (q, $J$ = 7.8 Hz, 2 H), 3.53 (m, 2 H), 4.07 (q, $J$ = 7.8 Hz, 2 H), 5.85 (t, $J$ = 2.0 Hz, 1 H), 7.39−7.42 (m, 3 H), 7.52−7.55 (m, 2 H). MS (CI/$NH_3$): *m/z* 341 ($M^+ + 1$, base).

**Preparation of Lactam Pyridine 33b (Scheme 2).** A mixture of phthalimide pyridine **9** (57 mg, 0.105 mmol) and anhydrous hydrazine (20 mg, 0.628 mmol) was stirred in 2 mL of absolute ethanol overnight at room temperature and then refluxed for 2 h. After the mixture cooled to room temperature, the solvent was removed, and the residue was separated using preparative TLC (silica 60; 1000 mm; Analtech, Newark, DE; petroleum ether−ethyl acetate (2:1)) to give 10 mg of the desired lactam (yield: 24%).

**Lactam (33b).** $^1$H NMR $\delta$: 1.01 (t, $J$ = 7.8 Hz, 3 H), 1.33 (t, $J$ = 7.8 Hz, 3 H), 2.05 (m, 2 H), 2.85 (t, $J$ = 6.9 Hz, 2 H), 3.07 (t, $J$ = 7.8 Hz, 2 H), 3.15 (m, 2 H), 4.13 (q, $J$ = 7.8 Hz, 2 H), 6.31 (m, 1 H), 7.43 (m, 3 H), 7.61−7.63 (m, 2 H). MS (CI/$NH_3$): *m/z* 356 ($M^+ + NH_4$), 339 ($M^+ + 1$).

**Preparation of Thiolactones 34 and 35 (Scheme 2).**[44] Under $N_2$, at room temperature, to a stirred solution of **23** or

**15** (50 mg, 0.109 mmol) in anhydrous methanol (5 mL) was added solid sodium thiomethoxide (7.6 mg, 0.109 mmol). The reaction reached completion (TLC) after stirring for 30 min. The solvent was removed, and the residue was purified by preparative TLC (silica 60; 1000 or 2000 mm; Analtech, Newark, DE; petroleum ether−ethyl acetate (9:1)) to give 38 mg of **34** (yield: 98%) and 38 mg of **35** (yield: 98%).

**3,4-Thiolactone (34).** $^1$H NMR $\delta$: 0.66 (t, $J$ = 7.8 Hz, 3 H), 1.33 (t, $J$ = 7.8 Hz, 3 H), 1.40 (m, 2 H), 2.71−3.06 (m, 4 H), 4.02 (t, $J$ = 7.8 Hz, 2 H), 7.41−7.43 (m, 3 H), 7.59−7.61 (m, 2 H). MS (CI/$NH_3$): $m/z$ 374 ($M^+ + NH_4$), 356 ($M^+ + 1$).

**2,3-Thiolactone (35).** $^1$H NMR $\delta$: 0.96 (t, $J$ = 6.9 Hz, 3 H), 1.00 (t, $J$ = 6.9 Hz, 3 H), 1.61 (m, 2 H), 2.65 (m, 2 H), 3.00 (t, $J$ = 6.6 Hz, 2 H), 3.12 (t, $J$ = 6.6 Hz, 2 H), 4.11 (q, $J$ = 6.9 Hz, 2 H), 7.42−7.44 (m, 3 H), 7.59 (m, 2 H). MS (CI/$NH_3$): $m/z$ 356 ($M^+ + 1$, base).

**General Procedure for Preparation of $\beta$-Amino-$\alpha,\beta$-unsaturated esters (36) (Scheme 9).** A $\beta$-ketoester (**38i−m**, **46**, 3 mmol) and ammonium acetate (4.5 mmol) were mixed in 5 mL of absolute ethanol and refluxed at 80 °C for 24 h. The solvent was removed, and the residue was chromatographed by preparative TLC to give the desired compounds in moderate yields.

**(3-Hydroxylpropyl) 3-Amino-3-phenyl-2-propenoate (36c).** $^1$H NMR $\delta$: 1.86−1.93 (m, 2 H), 3.71 (t, $J$ = 6.0 Hz, 2 H), 4.32 (t, $J$ = 6.0 Hz, 2 H), 4.97 (s, 1 H), 7.39−7.46 (m, 3 H), 7.53−7.56 (m, 2 H). MS (CI/$NH_3$): $m/z$ 240 ($MH^+ + NH_4$), 222 ($M^+ + 1$, base).

**(2,2,3,3,3-Pentafluoropropyl) 3-Amino-3-phenyl-2-propenoate (36d).** $^1$H NMR $\delta$: 4.60 (t, $J$ = 12.6 Hz, 2 H), 5.03 (s, 1 H), 7.44−7.49 (m, 3 H), 7.55−7.57 (m, 2 H). MS (CI/$NH_3$): $m/z$ 313 ($M^+ + NH_4$), 296 ($M^+ + 1$, base).

**Propyl 3-Amino-3-(2-fluorophenyl)-2-propenoate (36e).** $^1$H NMR $\delta$: 0.97 (t, $J$ = 7.8 Hz, 3 H), 1.69 (m, 2 H), 4.08 (t, $J$ = 6.9 Hz, 2 H), 4.91 (s, 1 H), 7.10−7.21 (m, 2 H), 7.39 (m, 1 H), 7.49 (m, 1 H). MS (CI/$NH_3$): $m/z$ 224 ($M^+ + 1$, base).

**Propyl 3-Amino-3-(3-fluorophenyl)-2-propenoate (36f).** $^1$H NMR $\delta$: 0.98 (t, $J$ = 7.8 Hz, 3 H), 1.69 (m, 2 H), 4.09 (t, $J$ = 6.9 Hz, 2 H), 4.97 (s, 1 H), 7.10−7.43 (m, 4 H). MS (CI/$NH_3$): $m/z$ 224 ($M^+ + 1$, base).

**Propyl 3-Amino-3-(4-fluorophenyl)-2-propenoate (36g).** $^1$H NMR $\delta$: 0.97 (t, $J$ = 7.8 Hz, 3 H), 1.66−1.73 (m, 2 H), 4.08 (t, $J$ = 6.9 Hz, 2 H), 4.94 (s, 1 H), 7.07−7.13 (m, 2 H), 7.52−7.57 (m, 2 H). MS (CI/$NH_3$): $m/z$ 224 ($M^+ + 1$, base).

**Preparation of 3-Phthalimidopropionaldehyde (37c) (Scheme 5).**[45] *N*-Carbethoxy-phthalimide (**53**, 4.384 g, 20 mmol), 3-amino-1-propanol (1.502 g, 20 mmol), and triethylamine (2.024 g, 20 mmol) were dissolved in THF (30 mL) and allowed to react for 6 h. The reaction mixture was evaporated, and the residue was purified by column chromatography (silica 60; petroleum ether−ethyl acetate (4:1)) to give 4.08 g of 3-phthalimido-1-propanol **54** (yield: 99%). $^1$H NMR ($CDCl_3$/TMS) $\delta$: 1.85−1.93 (m, 2 H), 3.63 (m, 2 H), 3.87 (t, $J$ = 6.9 Hz, 2 H), 7.73−7.75 (m, 2 H), 7.86−7.88 (m, 2 H). MS (CI/$NH_3$): $m/z$ 223 ($M^+ + NH_4$, base), 206 ($M^+ + 1$).

**Oxidation**.[46] A mixture of 3-phthalimido-1-propanol (**54**, 1.026 g, 5 mmol), PCC (2.156 g, 10 mmol), and silica gel (2.156 g) in 30 mL of dichloromethane was stirred at room temperature for 2 h. Ether (30 mL) was then added, and the reaction was filtered. After the solvent was removed, the residue was purified by preparative TLC (silica 60; 2000 mm; Analtech, Newark, DE; petroleum ether−ethyl acetate (4:1)) to give 0.629 g of the aldehyde **37c** (yield: 62%). $^1$H NMR ($CDCl_3$/TMS) $\delta$: 2.88 (t, $J$ = 6.9 Hz, 6 H), 3.85 (t, $J$ = 6.9 Hz, 2 H), 7.72−7.74 (m, 2 H), 7.81−7.87 (m, 2 H), 9.83 (s, 1 H). MS (EI): $m/z$ 203 ($M^+$), 175 ($MH^+ - CHO$), 160 ($M^+ - CH_2CHO$, base).

**Preparation of 3-Phthalimidobutyraldehyde (37d) (Scheme 5).**[45] The same conditions (for **54**) were used for preparing phthalimidoacetal **56** from *N*-carbethoxyphthalimide (**53**) and 4-aminobutyraldehyde diethylacetal (**55**). The yield for **56** was 95%. $^1$H NMR ($CDCl_3$/TMS) $\delta$: 1.19 (t, $J$ = 6.9 Hz, 6 H), 1.65−1.70 (m, 2 H), 1.72−1.77 (m, 2 H), 3.49 (m, 2 H), 3.62 (q, $J$ = 6.9 Hz, 2 H), 3.72 (t, $J$ = 6.9 Hz, 2 H), 4.52 (t, $J$ = 7.8 Hz, 1 H), 7.70−7.73 (m, 2 H), 7.83−7.85 (m, 2 H). MS (CI/$NH_3$): $m/z$ 309 ($M^+ + NH_4$), 217 ($M^+ - OEt - Et$, base).

A mixture of 3-phthaloyl-4-aminobutyraldehyde diethylacetal (**56**, 8.30 g, 28.5 mmol) and 1 N HCl (56 mL) in acetone (60 mL) was heated under reflux for 2 h. Acetone was removed, and the residue was extracted with ether (3 × 80 mL). The organic phase was washed with water, dried over $MgSO_4$, filtered, and the solvent removed by evaporation. The residue was column chromatographed (silica gel, petroleum ether−ethyl acetate (9:1)). $^1$H NMR ($CDCl_3$/TMS) $\delta$: 2.03 (m, 2 H), 2.54 (t, $J$ = 6.9 Hz, 2 H), 3.75 (t, $J$ = 6.9 Hz, 2 H), 7.70−7.76 (m, 2 H), 7.83−7.88 (m, 2 H), 9.78 (s, 1 H). MS (CI/$NH_3$): $m/z$ 217 ($M^+$, base).

**Preparation of $\beta$-Acetylthiopropionaldehyde (37e) (Scheme 5).**[47] The same condition (for acid **49**) was applied to prepare $\beta$-acetylthiopropionaldehyde (**37e**) from thiolacetic acid (2.13 g, 28 mmol) and acrolein (1.12 g, 1.34 mL, 20 mmol). The desired aldehyde **37e** (2.12 g) was obtained, yield: 80%. $^1$H NMR ($CDCl_3$/TMS) $\delta$: 2.34 (s, 3 H), 2.81 (t, $J$ = 6.9 Hz, 2 H), 3.12 (t, $J$ = 6.9 Hz, 2 H), 9.76 (s, 1 H). MS (CI/$NH_3$): $m/z$ 150 ($M^+ + NH_4$, base), 133 ($M^+ + 1$).

**Preparation of THP-Protected Aldehydes 37f and 37g (Scheme 5).**[43] A solution of 1,3-propanediol or 1,4-butanediol (30 mmol) and 3,4-dihydro-2*H*-pyran (30 mmol) in dry dichloromethane (25 mL) was cooled to 0 °C. Under stirring, PPTS (0.754 g, 3 mmol) was carefully added and allowed to react at the same temperature for 30 min before raising the temperature to room temperature. The reaction was then stirred for 4 h, the PPTS was filtered off, and the solvent was removed. Preparative TLC of the residue (silica gel, petroleum ether−ethyl acetate (4:1)) gave THP-protected alcohols, **57** (yield: 63%) or **58** (yield: 42%).

**For 57.** $^1$H NMR ($CDCl_3$/TMS) $\delta$: 1.53−1.60 (m, 4 H), 1.68−1.90 (m, 4 H), 3.53 (m, 1 H), 3.61 (m, 1 H), 3.80 (t, $J$ = 6.0 Hz, 2 H), 3.87 (m, 1 H), 3.95 (m, 1 H), 4.60 (s, 1 H). MS (CI/$NH_3$): $m/z$ 178 ($M^+ + NH_4$, base).

**For 58.** $^1$H NMR ($CDCl_3$/TMS) $\delta$: 1.53−1.86 (m, 10 H), 3.44 (m, 1 H), 3.51 (m, 1 H), 3.68 (t, $J$ = 6.9 Hz, 2 H), 3.78−3.90 (m, 2 H), 4.62 (t, $J$ = 3.0 Hz, 1 H). MS (CI/$NH_3$): $m/z$ 192 ($M^+ + NH_4$, base), 175 ($M^+ + 1$).

**Oxidation**.[48] A mixture of alcohol **57** or **58** (1 equiv), PCC (2 equiv), and sodium acetate (0.4 equiv.) in 10−30 mL of dichloromethane was stirred at room temperature for 2 h. Ether (30 mL) was then added, and the reaction was filtered. After the solvent was removed, the residue was purified by preparative TLC (silica 60; 2000 mm; Analtech, Newark, DE; petroleum ether−ethyl acetate (9:1)) to give THP-protected aldehyde, **37f**, in 83% yield or **37g** in 81% yield.

**For 37f.** $^1$H NMR ($CDCl_3$/TMS) $\delta$: 1.53−1.80 (m, 6 H), 2.70 (dt, $J$ = 6.0, 1.8 Hz, 2 H), 3.51 (m, 2 H), 3.85 (m, 2 H), 4.63 (t, $J$ = 3.9 Hz, 1 H), 9.83 (t, $J$ = 1.8 Hz, 1 H). MS (CI/$NH_3$): $m/z$ 176 ($M^+ + NH_4$, base).

**For 37g.** $^1$H NMR ($CDCl_3$/TMS) $\delta$: 1.54−1.88 (m, 6 H), 1.95 (m, 2 H), 2.55 (t, $J$ = 6.6 Hz, 2 H), 3.42 (m, 1 H), 4.49 (m, 1 H), 3.75−3.86 (m, 2 H), 4.57 (t, $J$ = 3.0 Hz, 1 H), 9.80 (s, 1 H). MS (CI/$NH_3$): $m/z$ 190 ($M^+ + NH_4$, base).

**Synthesis of $\beta$-Ketoesters 38 *via* Meldrum's Acids (Scheme 3)**.[23] The preparation of *S*-ethyl 3-oxothiovalerate (**38a**) is provided as an example. 2,2-Dimethyl-1,3-dioxane-4,6-dione (**43**, 0.721 g, 5 mmol) and propionyl chloride (0.509 g, 5.5 mmol) were dissolved in 10 mL of dry $CH_2Cl_2$. At 0 °C, 0.81 mL (0.791 g, 10 mmol) of pyridine (in the cases of aromatic acid chlorides, using 4-(dimethylamino)pyridine instead of pyridine) was then added dropwise. The reaction temperature was kept at 0 °C for 1 h and then raised to room temperature for an additional 1 h. The reaction mixture was washed with 1 N HCl (10 mL) and water (5 mL) and then dried with anhydrous $MgSO_4$. Removal of the solvent left the desired product (**44a**), which was directly used for the next reaction without purification.

Compound **44a** (670 mg, 3.35 mmol) and ethanethiol (0.621 g, 10 mmol) were mixed in 10 mL of toluene. This mixture was heated at 80 °C in a flask with an effective reflux

condenser for 24 h. The solvent and excess ethanethiol were removed, and the residue was purified by TLC (silica 60, petroleum ether−ethyl acetate (9:1)) to give the desired product 282 mg, yield: 53%.

***S*-Ethyl 3-Oxothiovalerate (38a).** $^1$H NMR $\delta$: 1.07 (t, $J$ = 6.9 Hz, 3 H), 1.28 (t, $J$ = 6.9 Hz, 3 H), 2.58 (q, $J$ = 6.9 Hz, 2 H), 2.94 (q, $J$ = 6.9 Hz, 2 H), 3.66 (s, 2 H). MS (CI/$NH_3$): $m/z$ 178 ($M^+ + NH_4$), 161 ($M^+ + 1$).

***S*-Hexyl 3-Oxothiovalerate (38b).** $^1$H NMR $\delta$: 0.88 (t, $J$ = 6.9 Hz, 3 H), 1.07 (t, $J$ = 7.8 Hz, 3 H), 1.26−1.41 (m, 6 H), 1.59 (m, 2 H), 2.58 (q, $J$ = 7.8 Hz, 2 H), 2.92 (t, $J$ = 6.9 Hz, 2 H), 3.66 (s, 2 H). MS (CI/$NH_3$): $m/z$ 234 ($M^+ + NH_4$, base), 217 ($M^+ + 1$).

***S*-(2,2,2-Trifluoroethyl) 3-Oxothiovalerate (38c).** $^1$H NMR $\delta$: 1.09 (t, $J$ = 7.8 Hz, 3 H), 2.58 (q, $J$ = 7.8 Hz, 2 H), 3.64 (q, $J$ = 9.9 Hz, 2 H), 3.76 (s, 2 H). MS (CI/$NH_3$): $m/z$ 232 ($M^+ + NH_4$, base), 214 ($M^+ + 1$).

***S*-(2-Tetrahydropyranyloxylethyl) 3-Oxothiovalerate (38d).** $^1$H NMR $\delta$: 1.07 (t, $J$ = 7.8 Hz, 3 H), 1.53−1.84 (m, 6 H), 2.58 (q, $J$ = 7.8 Hz, 2 H), 3.18 (t, $J$ = 6.9 Hz, 2 H), 3.49−3.62 (m, 2 H), 3.68 (s, 2 H), 3.82−3.90 (m, 2 H), 4.63 (m, 1 H). MS (CI/$NH_3$): $m/z$ 278 ($M^+ + NH_4$), 261 ($M^+ + 1$).

***S*-(3-Tetrahydropyranyloxylpropyl) 3-Oxothiovalerate (38e).** $^1$H NMR $\delta$: 1.07 (t, $J$ = 7.8 Hz, 3 H), 1.52−1.86 (m, 6 H), 1.91 (m, 2 H), 2.58 (q, $J$ = 7.8 Hz, 2 H), 3.04 (t, $J$ = 7.8 Hz, 2 H), 3.46 (m, 2 H), 3.67 (s, 2 H), 3.82 (m, 2 H), 4.58 (t, $J$ = 3.0 Hz, 1 H). MS (CI/$NH_3$): $m/z$ 292 ($M^+ + NH_4$, base).

***S*-((2,2-Dimethyl-1,3-dioxolan-4-yl)methyl) 3-Oxothiovalerate (38f).** $^1$H NMR $\delta$: 1.08 (t, $J$ = 6.9 Hz, 3 H), 1.34 (s, 3 H), 1.43 (s, 3 H), 2.57 (q, $J$ = 6.9 Hz, 2 H), 3.15 (dd, $J$ = 6.0, 3.0 Hz, 2 H), 3.67 (m, 1 H), 3.70 (s, 2 H), 4.08 (m, 1 H), 4.26 (m, 1 H). MS (CI/$NH_3$): $m/z$ 264 ($M^+ + NH_4$, base), 247 ($M^+ + 1$).

***S*-Ethyl 3-Oxothio(benzyloxylvalerate) (38g).** $^1$H NMR $\delta$: 1.27 (t, $J$ = 7.8 Hz, 3 H), 2.84 (t, $J$ = 6.9 Hz, 2 H), 2.92 (q, $J$ = 7.8 Hz, 2 H), 3.70 (s, 2 H), 3.75 (t, $J$ = 6.9 Hz, 2 H), 4.51 (s, 2 H), 7.33 (m, 5 H). MS (CI/$NH_3$): $m/z$ 284 ($M^+ + NH_4$, base), 267 ($M^+ + 1$).

***S*-Ethyl 3-Oxothio(acetylthiovalerate) (38h).** $^1$H NMR $\delta$: 1.27 (t, $J$ = 7.8 Hz, 3 H), 2.32 (s, 3 H), 2.91 (q, $J$ = 7.8 Hz, 2 H), 2.94 (t, $J$ = 6.9 Hz, 2 H), 3.07 (t, $J$ = 6.9 Hz, 2 H), 3.66 (s, 2 H). MS (CI/$NH_3$): $m/z$ 252 ($M^+ + NH_4$, base), 235 ($M^+ + 1$).

**(2,2,3,3,3-Pentafluoropropyl) Benzoyl Acetate (38j).** $^1$H NMR $\delta$: 4.12 (s, 2 H), 4.64 (t, $J$ = 12.6 Hz, 2 H), 7.43−7.66 (m, 3 H), 7.92−7.98 (m, 2 H). MS (CI/$NH_3$): $m/z$ 314 ($M^+ + NH_4$, base), 297 ($M^+ + 1$).

**Propyl *o*-Fluorobenzoyl Acetate (38k).** $^1$H NMR $\delta$: 0.90 (t, $J$ = 7.8 Hz, 3 H), 1.64 (m, 2 H), 4.00 (s, 2 H), 4.12 (t, $J$ = 6.9 Hz, 2 H), 7.13 (m, 1 H), 7.25 (m, 1 H), 7.57 (m, 1 H), 7.91 (m, 1 H). MS (CI/$NH_3$): $m/z$ 242 ($M^+ + NH_4$, base), 225 ($M^+ + 1$).

**Propyl *m*-Fluorobenzoyl Acetate (38l).** $^1$H NMR $\delta$: 0.90 (t, $J$ = 7.8 Hz, 3 H), 1.64 (m, 2 H), 3.98 (s, 2 H), 4.12 (t, $J$ = 6.9 Hz, 2 H), 7.31 (m, 1 H), 7.47 (m, 1 H), 7.65 (d, $J$ = 6.9 Hz, 1 H), 7.73 (d, $J$ = 6.9 Hz, 1 H). MS (CI/$NH_3$): $m/z$ 242 ($M^+ + NH_4$, base).

**Propyl *p*-Fluorobenzoyl Acetate (38m).** $^1$H NMR $\delta$: 0.90 (t, $J$ = 7.8 Hz, 3 H), 1.61−1.72 (m, 2 H), 3.98 (s, 2 H), 4.12 (t, $J$ = 6.9 Hz, 2 H), 7.11−7.19 (m, 2 H), 7.97−8.02 (m, 2 H). MS (CI/$NH_3$): $m/z$ 242 ($M^+ + NH_4$, base), 225 ($M^+ + 1$).

To prepare compound **46**, a transesterification reaction was used. Ethyl benzoyl acetate (**45**, 1.92 g, 10 mmol) and 1,3-propanediol (0.761 g, 10 mmol) in toluene (10 mL) were heated with stirring for 24 h. The solvent was removed, and the residue was column chromatographed (silica 60, petroleum ether−ethyl acetate (3:1)) to give 1.67 g of the desired product, yield: 75%.

**Hydroxylpropyl Benzoyl Acetate (46).** $^1$H NMR $\delta$: 1.87 (m, 2 H), 3.69 (t, $J$ = 6.0 Hz, 2 H), 4.03 (s, 2 H), 4.34 (t, $J$ = 6.0 Hz, 2 H), 7.43−7.52 (m, 2 H), 7.58−7.64 (m, 1 H), 7.92−7.96 (m, 2 H). MS (CI/$NH_3$): $m/z$ 240 ($M^+ + NH_4$, base), 223 ($M^+ + 1$).

**Preparation of $\beta$-Benzyloxylpropionyl Chloride (42b) (Scheme 4).**[49] $\beta$-Propiolactone (**47**, 2.16 g, 30 mmol) and benzyl alcohol (19.5 g, 80 mmol) were stirred at 75 °C for 24 h. After the mixture cooled to room temperature, 60 mL of 1 N NaOH was carefully added to the reaction mixture, which was stirred for 1 h and then extracted with dichloromethane (3 × 40 mL). The aqueous phase was acidified with 80 mL of 1 N HCl, extracted with ether (3 × 80 mL), dried over $MgSO_4$, and filtered. Removal of the solvent left a viscous oil (**48**), 4.91 g, yield: 91%. $^1$H NMR ($CDCl_3$/TMS) $\delta$: 2.67 (t, $J$ = 6.9 Hz, 2 H), 3.76 (t, $J$ = 6.9 Hz, 2 H), 4.56 (s, 2 H), 7.34 (m, 5 H). MS (CI/$NH_3$): $m/z$ 180 ($M^+$).

Acid **48** (4.90 g, 27 mmol) and thionyl chloride (6.42 g, 54 mmol) were mixed carefully under $N_2$ while cooling in an ice bath. After the gas evolution stopped, the mixture was refluxed for 2 h. The excess thionyl chloride was removed by vacuum leaving compound **42b**, which was used directly in the next step.

**Preparation of $\beta$-Acetylthiopropionyl Chloride (42c) (Scheme 4).**[50] Under ice-cooling conditions, 3 mL (42 mmol) of thiolacetic acid was added very carefully to acrylic acid (2.16 g, 30 mmol). After the mixture was stirred and cooled for 1 h, the temperature was allowed to rise to 25 °C, and stirring continued overnight. Removing all volatile materials gave 2.36 g of the acid **49**, yield: 53%.

To prepare $\beta$-acetylthiopropionyl chloride (**42c**), the same condition (for **42b**) was adopted using acid **49**.

**Preparation of THP-Protected Thiols 50 and 51 (Scheme 4).**[43] A solution of 2-mercaptoethanol or 3-mercapto-1-propanol (30 mmol) and 3,4-dihydro-2*H*-pyran (30 mmol) in dry dichloromethane (25 mL) was cooled to 0 °C. While the mixture was being stirred, 3 mmol of PPTS was carefully added, and the reaction mixture was left at the same temperature for 30 min before returning to room temperature. The reaction was then stirred for 4 h, the PPTS was filtered off, and the solvent was removed. Chromatography of the residue (silica gel, petroleum ether−ethyl acetate (9:1)) gave the desired thiol **50** (yield: 60%) or **51** (yield: 81%).

**For 50**. $^1$H NMR ($CDCl_3$/TMS) $\delta$: 1.52−1.88 (m, 6 H), 1.72 (t, $J$ = 3.9 Hz, 1 H), 2.73 (dt, $J$ = 6.9, 3.9 Hz, 2 H), 3.49−3.60 (m, 2 H), 3.83−3.93 (m, 2 H), 4.65 (t, $J$ = 3.0 Hz, 1 H). MS (CI/$NH_3$): $m/z$ 180 ($M^+ + NH_4$).

**For 51.** $^1$H NMR ($CDCl_3$/TMS) $\delta$: 1.39 (t, $J$ = 7.8 Hz, 1 H), 1.52−1.59 (m, 4 H), 1.68−1.83 (m, 2 H), 1.86−1.95 (m, 2 H), 2.65 (dt, $J$ = 6.9, 7.8 Hz, 2 H), 3.50 (m, 2 H), 3.85 (m, 2 H), 4.59 (t, $J$ = 3.9 Hz, 1 H). MS (CI/$NH_3$): $m/z$ 194 ($M^+ + NH_4$), 177 ($M^+ + 1$).

**Preparation of Thiol 52 (Scheme 4).** 3-Mercapto-1,2-propanediol (2.16 g, 20 mmol), PPTS (0.503 g, 2 mml), and anhydrous $MgSO_4$ (2 g) were dissolved in 20 mL of dry acetone. The reaction mixture was stirred at room temperature for 2 days. Solid materials were filtered off. The filtrate was evaporated, and the residue was separated with preparative TLC (silica 60; 2000 mm; Analtech, Newark, DE; petroleum ether−ethyl acetate (9:1)) to give 2.01 g of thiol **52** (yield: 68%). $^1$H NMR ($CDCl_3$/TMS) $\delta$: 1.37 (s, 3 H), 1.44 (s, 3 H), 1.48 (t, $J$ = 7.8 Hz, 1 H), 2.61 (m, 1 H), 2.75 (m, 1 H), 3.77 (m, 1 H), 4.09−4.23 (m, 2 H).

**Molecular Modeling.** All calculations were performed on a Silicon Graphics Indigo 2 R8000 workstation.

The MRS 1476 model was constructed using the "Sketch Molecule" of SYBYL 6.4.2.[29] Semiempirical molecular orbital calculations were done using the AM1 Hamiltonian[21] as implemented in MOPAC 6.0[30] (keywords: PREC, GNORM = 0.1, EF, MMOK if necessary).

The three-dimensional human $A_3$ receptor model was built and optimized using SYBYL 6.4.2 and Macromodel 5.0,[32] respectively, based on the approach described by Moro et al.[25] Briefly, the seven transmembrane helical domains were identified with the aid of Kyte-Doolittle hydrophobicity[33] and $E_{mini}$[33] surface probability parameters. The helices were built and energy minimized for each transmembrane sequence. The minimized helices were then grouped together to form a helical bundle matching the overall characteristics of the electron

density map of rhodopsin. The helical bundle was energy-minimized using the AMBER[34] all-atom force field, until the root mean square value of the conjugate gradient (CG) was <0.1 kcal/mol/Å. A fixed dielectric constant of 4.0 was used throughout these calculations.

The MRS 1476 structure was rigidly docked into the helical bundle using graphical manipulation with continuous energy monitoring (Dock module of SYBYL). The manually docked local energy minimized receptor−ligand complexes were subjected to an additional conjugate gradient minimization run of 300 steps. Partial atomic charges for the ligands were taken from the MOPAC output files. A fixed dielectric constant of 4.0 was used throughout the docking calculations. We have recently introduced the *cross-docking* procedure to obtain energetically refined structures of GPCR−ligand complexes.[25] We applied this technique to predict the structure of the MRS 1476−$A_3$ receptor complex. Cross docking allows possible ligand-induced rearrangements of the 7TM bundle to be explored by sampling 7TM conformations in the presence of the docked ligands. Small translations and rotations were applied to each helix relative to its original position until a new lower energy geometry was obtained. These manual adjustments were followed by 25 ps of molecular dynamics (MD module of Macromodel) performed at a constant temperature of 300 K using a time step of 0.001 ps and a dielectric constant of 4.0. This procedure was followed by another sequence of CG energy minimization to a gradient threshold of <0.1 kcal/mol/Å. Energy minimization of the complexes was performed using the AMBER all-atom force field in MacroModel.

**CoMFA Analysis.** CoMFA[18] is a three-dimensional QSAR method that operates on a set of ligands that have been superimposed to reflect their anticipated common binding orientation. CoMFA models describe the extent to which the change in magnitude of the electrostatic and steric fields as a function of compound, sampled as a function of spatial position around the compound set, accounts for the variance in measured biological activity. The CoMFA study was performed using SYBYL 6.4.2,[29] and quantum calculations used throughout this study were performed using MOPAC (Ver. 6.0)[31] and Gaussian 94.[35]

**Data Set and Molecular Superposition.** A total of 41 pyridine derivatives were included in the training set used to generate the CoMFA model for $A_3$ receptors (see Tables 1 and 6). The synthesis and binding affinity constants of **65**−**87** pyridine derivatives were reported in detail previously.[16]

The pyridine moiety and the two ester groups at 3- and 5-positions are believed to be a key determinant of binding interactions of pyridine derivatives. Therefore, the ligands in this study were superimposed on both the pyridine nucleus and the carbonyl of the 3- and 5-ester groups by fitting a minimum energy conformation of the compound **6** (reference structure). The low-energy conformer of compound **6** was predicted in a previous study.[16] All the other compounds were fitted by a least squares algorithm to the reference structure so as to maximally align their substituents with the corresponding substituents of the reference structure. The substituents at the meta position of the 6-phenyl ring were aligned using the best fit inside the hydrophobic cavity of the human $A_3$ receptor, as reported.[19] The fitted conformations of each compound were fully minimized using MOPAC (AM1 Hamiltonian, keywords: PREC, GNORM=0.01, EF).

**Atomic Charge Calculations.** Partial atomic charges are required for calculating electrostatic fields in CoMFA. Partial atomic charges for compound **6** were calculated at the semiempirical level using the MNDO,[36] AM1, and PM3[37] Hamiltonians of MOPAC. The results of each method were compared to those obtained using the RHF/6-31G(*)//RHF/3-21G(*) ab initio level of Gaussian 94. The charges derived from electrostatic potentials[38] and calculated using AM1 were found to agree best with the ab initio charges. Therefore, partial atomic charges for all the pyridine derivatives were calculated using the AM1 Hamiltonian.

**CoMFA Field Calculations and Regression Techniques.** The electrostatic and steric fields were sampled along a three-dimensional lattice encompassing all molecules in each receptor data set. The lattice consisted of 9261 sample points based on a 1.0 Å lattice spacing with boundaries extending 2.0 Å beyond the largest structure in all directions. The 2.00, 1.50, and 1.25 Å lattice spacing was found not to improve the CoMFA results. The lattice points within the union volume of the superimposed structures were dropped. The probe used to calculate the CoMFA fields consisted of an $sp^3$ carbon atom with a +1 charge and a van der Waals radius of 1.52 Å. The steric and electrostatic fields were calculated separately for each molecule using a Lennard-Jones 6−12 potential and a Coulombic potential with a $1/r$ distance-dependent dielectric. The steric and electrostatic energies were truncated at 30 kcal/mol. The field values corresponding to the 9261 sample points for each molecule, together with binding affinity data, were stored in a SYBYL Molecular Spreadsheet to facilitate statistical analysis.

Partial least-squares (PLS) regression analysis[39] was performed on the pyridine data sets using a subset of the CoMFA field sample points falling within a standard deviation of ≤1.0 kcal/mol. The steric and the electrostatic fields were scaled to equalize their weighting in the CoMFA models (SYBYL command "scaling CoMFA_std"). PLS was performed using cross-validation to evaluate the predictive ability of the CoMFA models.[40] The optimal number of latent variables was derived from the cross-validation equation having the lowest standard error, and a significance level of ≥99.5% was estimated using the stepwise F-test. Bootstrap analysis[40] of the data set was used to evaluate the statistical confidence limits of the results. A $s$ value of 2.0 was adopted for both the cross-validated and non-cross-validated analysis. The $s$ values of 1.0 or 0.5 did not significantly change the calculated $r^2$.

Initial PLS analyses were performed in conjunction with the cross-validation (leave-one-out method) option to obtain the optimal number of components to be used in the subsequent analyses of the data set. The PLS analysis was repeated with the number of cross-validation groups set to zero. The optimal number of components was designated as that which yielded the highest cross-validated $r^2$ values in the non-cross-validated (conventional) analyses. The final PLS analysis with 10 bootstrap groups and the optimal number of components was performed on the complete data set.

The corresponding calibration equation (resulting from the simultaneous contribution of all the observations) was derived after the optimal dimensionality of each receptor model was established, by PLS analysis and cross-validation. The calibration equation with latent variables was then converted to the original parametric space represented by probe−ligand interaction energies. A 3D-QSAR was therefore derived whose coefficients were associated with statistically significant lattice locations. CoMFA coefficient contour maps were generated by interpolation of the pairwise products between the 3D-QSAR coefficients and the standard deviations of the associated energy variables.

**The Test Set.** The test set consisted of three molecules (**10**, **24**, and **27**, see Table 4). These structures were chosen to maximize a uniform sampling of biological activity. All predicted activities for the test set molecules were calculated using the optimized CoMFA model. The results of the non-cross-validated calibration model on the test sets are summarized in Table 5.

**"Predictive" $r^2$ Values.** The "predictive" $r^2_{pred}$ was based only on molecules not included in the training set and is defined as explained by Marshall and co-workers.[41]

**Pharmacology. Radioligand Binding Studies.** Binding of [$^3$H]*R*-$N^6$-phenylisopropyladenosine ([$^3$H]*R*-PIA) to $A_1$ receptors from rat cerebral cortex membranes and of [$^3$H]-2-[4-[(2-carboxyethyl)phenyl]ethylamino]-5′-*N*-ethylcarbamoyladenosine ([$^3$H]CGS 21680) to $A_{2A}$ receptors from rat striatal membranes was performed as described previously.[20,21]

Adenosine deaminase (3 units/mL) was present during the preparation of the brain membranes, in a preincubation of 30 min at 30 °C, and during the incubation with the radioligands.

Binding of [$^{125}$I]$N^6$-(4-amino-3-iodobenzyl)-5′-*N*-methylcarbamoyladenosine ([$^{125}$I]AB-MECA) to membranes prepared from HEK-293 cells stably expressing the human $A_3$ receptor, clone HS-21a (Receptor Biology, Inc., Baltimore MD), or to membranes prepared from CHO cells stably expressing the rat $A_3$ receptor was performed as described.[22] The assay medium consisted of a buffer containing 10 mM $Mg^{2+}$, 50 mM Tris, and 1 mM EDTA, at pH 8.0. The glass incubation tubes contained 100 mL of the membrane suspension (0.3 mg protein/mL, stored at −80 °C in the same buffer), 50 mL of [$^{125}$I]AB-MECA (final concentration 0.3 nM), and 50 mL of a solution of the proposed antagonist. Nonspecific binding was determined in the presence of 100 mM $N^6$-phenylisopropyladenosine (*R*-PIA).

All nonradioactive compounds were initially dissolved in DMSO and diluted with buffer to the final concentration, where the amount of DMSO never exceeded 2%.

Incubations were terminated by rapid filtration over Whatman GF/B filters, using a Brandell cell harvester (Brandell, Gaithersburg, MD). The tubes were rinsed three times with 3 mL of buffer each.

At least five different concentrations of competitor, spanning 3 orders of magnitude adjusted appropriately for the $IC_{50}$ of each compound, were used. $IC_{50}$ values, calculated with the nonlinear regression method implemented in the InPlot program (Graph-PAD, San Diego, CA), were converted to apparent $K_i$ values using the Cheng-Prusoff equation[42] and $K_d$ values of 1.0 nM ([$^3$H]*R*-PIA); 14 nM ([$^3$H]CGS 21680); and 0.59 and 1.46 nM ([$^{125}$I]AB-MECA at human and rat $A_3$ receptors, respectively).

## Abbreviations

[$^{125}$I]AB-MECA, [$^{125}$I]$N^6$-(4-amino-3-iodobenzyl)-5′-*N*-methylcarbamoyladenosine; CGS 21680, 2-[4-[(2-carboxyethyl)phenyl]ethyl-amino]-5′-*N*-ethylcarbamoyladenosine; CHO cells, Chinese hamster ovary cells; CoMFA, comparative molecular field analysis; DMAP, *N*,*N*-dimethylaminopyridine; DMSO, dimethyl sulfoxide; DAST, diethylaminosulfur trifluoride; DPPA, diphenylphosphoryl azide; EDAC, 1-ethyl-3-(3-dimethylaminopropyl)carbodiimide; HEK cells, human embryonic kidney cells; IB-MECA, $N^6$-(3-iodobenzyl)-5′-*N*-methylcarbamoyladenosine; $K_i$, equilibrium inhibition constant; MRS 1191, 3-ethyl 5-benzyl 2-methyl-6-phenyl-4-phenylethynyl-1,4-(±)-dihydropyridine-3,5-dicarboxylate; MRS 1476, 2,3,4,5-tetraethyl-6-phenylpyridine-3-thiocarboxylate-5-carboxylate; MRS 1523, 2,3-ethyl-4,5-dipropyl-6-phenylpyridine-3-thiocarboxylate-5-carboxylate; PCC, pyridinium chlorochromate; PLS, partial least squares; PPTS, pyridinium *p*-toluenesulfonate; *R*-PIA, *R*-$N^6$-phenylisopropyladenosine; SAR, structure−activity relationship; SEAL, steric and electrostatic alignment; TBAF, tetrabutylammonium fluoride; THP, tetrahydropyranyl; TM, transmembrane helical domain; Tris, tris(hydroxymethyl)aminomethane.

**Acknowledgment.** We thank Prof. Gary L. Stiles and Dr. Mark E. Olah (Duke University, Durham, NC) for providing cells expressing recombinant $A_3$ receptors. We thank Kristie Calvert for technical assistance.

**Supporting Information Available:** Schemes 6−9 and coordinate files for the models of the complex of MRS 1476 with the human $A_3$ receptor. This material is available free of charge via the Internet at http://pubs.acs.org.

## References

(1) Jacobson, K. A. $A_3$ adenosine receptors: Novel ligands and paradoxical effects. *Trends Pharmacol. Sci*. **1998**, *19*, 184−191.
(2) Beaven, M. A.; Ramkumar, V.; Ali, H. Adenosine-$A_3$ receptors in mast-cells. *Trends Pharmacol. Sci*. **1994**, *15*, 13−14.
(3) Knight, D.; Zheng, X.; Rocchini, C.; Jacobson, M. A.; Bai, T.; Walker, B. Adenosine $A_3$ receptor stimulation inhibits migration of human eosinophils. *J. Leukoc. Biol*. **1997**, *62*, 465−468.
(4) von Lubitz, D. K. J. E.; Lin, R. C. S.; Popik, P.; Carter, M. F.; Jacobson, K. A. Adenosine $A_3$ receptor stimulation and cerebral ischemia. *Eur. J. Pharmacol*. **1994**, *263*, 59−67.
(5) von Lubitz, D. K. J. E.; Lin, R. C. S.; Jacobson, K. A. Adenosine $A_3$ receptor antagonists and protection cerebral ischemic damage in gerbils. *Soc. Neurosci*. **1997**, *23*, Abstr. 745.16, 1924.
(6) Jacobson, K. A.; Kim, H. O.; Siddiqi, S. M.; Olah, M. E.; Stiles, G.; von Lubitz, D. K. J. E. $A_3$ adenosine receptors: design of selective ligands and therapeutic prospects. *Drugs of the Future*, **1995**, *20*, 689−699.
(7) Salvatore, C. A.; Jacobson, M. A.; Taylor, H. E.; Linden, J.; Johnson, R. G. Molecular cloning and characterization of the human $A_3$ adenosine receptor. *Proc. Natl. Acad. Sci. U.S.A*. **1993**, *90*, 10365−10369.
(8) Linden, J.; Taylor, H. E.; Robeva, A. S.; Tucker, A. L.; Stehle, J. H.; Rivkees, S. A.; Fink, J. S.; Reppert, S. M. Molecular-Cloning and Functional Expression of a Sheep-$A_3$ Adenosine Receptor With Widespread Tissue Distribution. *Mol. Pharmacol*. **1993**, *44*, 524−532.
(9) Ji, X.-d.; von Lubitz, D.; Olah, M. E.; Stiles, G. L.; Jacobson, K. A. Species differences in ligand affinity at central $A_3$-adenosine receptors. *Drug Dev. Res*. **1994**, *33*, 51−59.
(10) van Rhee, A. M.; Jiang, J. L.; Melman, N.; Olah, M. E.; Stiles, G. L.; Jacobson, K. A. Interaction of 1,4-dihydropyridine and pyridine-derivatives with adenosine receptors − selectivity for $A_3$ receptors. *J. Med. Chem*. **1996**, *39*, 2980−2989.
(11) Jiang, J.-l.; van Rhee, A. M.; Melman, N.; Ji, X.d.; Jacobson, K. A. 6-Phenyl-1,4-dihydropyridine derivatives as potent and selective $A_3$ adenosine receptor antagonists. *J. Med. Chem*. **1996**, *39*, 4667−4675.
(12) Jiang, J.-l.; van Rhee, A. M.; Chang, L.; Patchornik, A.; Evans, P.; Melman, N.; Jacobson, K. A. Structure activity relationships of 4-phenylethynyl-6-phenyl-1,4-dihydropyridines as highly selective $A_3$ adenosine receptor antagonists. *J. Med. Chem*. **1997**, *40*, 2596−2608.
(13) Kim, Y.-C.; de Zwart, M.; Chang, L.; Moro, S.; von Frijtag Drabbe Künzel, J. K.; Melman, N.; IJzerman, A. P.; Jacobson, K. A. Derivatives of the triazoloquinazoline adenosine antagonist (CGS15943) having high potency at the human $A_{2B}$ and $A_3$ receptor subtypes. *J. Med. Chem*. **1998**, *41*, 2835−2841.
(14) Karton, Y.; Jiang, J. L.; Ji, X. D.; Melman, N.; Olah, M. E.; Stiles, G. L.; Jacobson, K. A. Synthesis and biological-activities of flavonoid derivatives as as adenosine receptor antagonists. *J. Med. Chem*. **1996**, *39*, 2293−2301.
(15) Jacobson, M. A.; Chakravarty, P..K.; Johnson, R. G.; Norton, R. Novel selective nonxanthine selective $A_3$ adenosine receptor antagonists. *Drug Dev. Res*. **1996**, 37, 131.
(16) Li, A.-H.; Moro, S.; Melman, N.; Ji, X.-d.; Jacobson, K. A. Structure activity relationships and molecular modeling of 3,5-diacyl-2,4-dialkylpyridine derivatives as selective $A_3$ adenosine receptor antagonists. *J. Med. Chem*. **1998**, *41*, 3186−3201.
(17) Van Muijlwijk-Koezen, J. E.; Timmerman, H.; Link, R.; Van der Goot, H.; Ijzerman, A. P. A novel class of adenosine $A_3$ receptor ligands. II. Structure affinity profile of a series of isoquinoline and quinazolinecompounds. *J. Med. Chem*. **1998**, *41*, 3994−4000.
(18) Cramer III, R. D.; Patterson, D. E.; Bunce, J. D. Comparative molecular field analysis (CoMFA). 1. Effect of shape on binding of steroids to carrier proteins. *J. Am. Chem. Soc*. **1988**, *110*, 5959−5967.
(19) Moro, S.; Li, A. H.; Jacobson, K. A. Molecular modeling studies of human $A_3$ adenosine receptor antagonists: structural homology and receptor docking. *J. Chem. Inf. Comput. Sci*. **1998**, *38*, 1239−1248.
(20) Schwabe, U.; Trost, T. Characterization of adenosine receptors in rat brain by (−) [$^3$H]N$^6$-phenylisopropyladenosine. *Naunyn-Schmiedeberg's Arch. Pharmacol*. **1980**, *313*, 179−187.
(21) Jarvis, M. F.; Schutz, R.; Hutchison, A. J.; Do, E.; Sills, M. A.; Williams, M. [$^3$H]CGS 21680, an $A_2$ selective adenosine receptor agonist directly labels $A_2$ receptors in rat brain tissue. *J. Pharmacol. Exp. Ther*. **1989**, *251*, 888−893.
(22) Olah, M. E.; Gallo-Rodriguez, C.; Jacobson, K. A.; Stiles, G. L. [$^{125}$I]AB-MECA, a high affinity radioligand for the rat $A_3$ adenosine receptor. *Mol. Pharmacol*. **1994**, *45*, 978−982.
(23) Oikawa, Y.; Sugano, K.; Yonemitsu, O. Meldrum's acid in Organic Synthesis. 2. General and Versatile Synthesis of β-Keto Esters. *J. Org. Chem*. **1978**, *43*, 2087−2088.

(24) Moro, S.; van Rhee, A. M.; Sanders, L. H.; Jacobson, K. A. Flavonoid derivatives as adenosine receptor antagonists: A comparison of the hypothetical binding sites based on a comparative molecular field analysis model. *J. Med. Chem.* **1998**, *41*, 46−52.
(25) Moro, S.; Guo, D.; Camaioni, E.; Boyer, J. L.; Harden K. T.; Jacobson, K. A. Human $P2Y_1$ receptor: molecular modeling and site-directed mutagenesis as tools to identify agonist and antagonist recognition sites. *J. Med. Chem.* **1998**, *41*, 1456−1466.
(26) Gouldson. P. R.; Snell, C. R.; Reynolds, C. A. A new approach to docking in the $\beta_2$-adrenergic receptor that exploits the domain structure of G protein-coupled receptors. *J. Med. Chem.* **1997**, *40*, 3871−3886.
(27) Schertler, G. F.; Villa, C.; Henderson, R. Projection structure of rhodopsin. *Nature* **1993**, *362*, 770−772.
(28) Urger, V. M.; Hargrave, P. A.; Baldwin, J. M.; Schertler, G. F. X. Arrangement of rhodopsin transmenbrane a-helices. *Nature* **1997**, *389*, 203−206.
(29) The program SYBYL 6.3 is available from TRIPOS Associates, St. Louis, MO, 1993.
(30) Dewar, M. J. S. E.; Zoebisch, G.; Healy, E. F. AM1: A New General Purpose Quantum Mechanical Molecular Model. *J. Am. Chem. Soc.* **1985**, *107*, 3902−3909.
(31) MOPAC 6.0 is available from Quantum Chemistry Program Exchange.
(32) Mohamadi, F.; Richards, N. G. J.; Guida, W. C.; Liskamp, R.; Lipton, M.; Caufield, C.; Chang, G.; Hendrickson, T.; Still, W. C. MacroModel-An Integrated Software System for Modeling Organic and Bioorganic Molecules using Molecular Mechanics. *J. Comput. Chem.* **1990**, *11*, 440−450.
(33) Kyte, J.; Doolittle, R. F. A simple method for displaying the hydrophobic character of a protein. *J. Mol. Biol.* **1982**, *157*, 105−132.
(34) Weiner, S. J.; Kollman, P. A.; Nguyen, D. T.; Case, D. A. An all-atom force field for simulation of protein and nucleic acids. *J. Comput. Chem.* **1986**, *7*, 230−252.
(35) Frisch, M. J.; Trucks, G. W.; Schlegel, H. B.; Gill, P. M. W.; Johnson, B. G.; Robb, M. A.; Cheeseman, J. R.; Keith, T.; Petersson, G. A.; Montgomery, J. A.; Raghavachari, K.; Al-Laham, M. A.; Zakrzewski, V. G.; Ortiz, J. V.; Foresman, J. B.; Cioslowski, J.; Stefanov, B. B.; Nanayakkara, A.; Challacombe, M.; Peng, C. Y.; Ayala, P. Y.; Chen, W.; Wong, M. W.; Andres, J. L.; Replogle, E. S.; Gomperts, R.; Martin, R. L.; Fox, D. J.; Binkley, J. S.; Defrees, D.; Baker, J. J.; Stewart, J. P.; Head-Gordon, M.; Gonzalez, C.; Pople, J. A. *Gaussian 94, Revision C.2*; Gaussian, Inc., Pittsburgh, PA, 1995. Dobbs, K. D.; Hehre, W. J. Molecular orbital theory of the properties of inorganic and organometallic compounds 5. Extended basis sets for first-row transition metals. *J. Comput. Chem.* **1987**, *8*, 861−879.
(36) Stewart, J. J. P. Optimization of Paramiters for Semiempirical Methods I. Methods. *J. Comput. Chem.* **1989**, *10*, 209−217.
(37) Dewar, M. J. S.; Thiel, W. Ground States of Molecules. 38. The MNDO method. Approximations and Parameters. *J. Am. Chem. Soc.* **1977**, *99*, 4899−4905.
(38) Chirlian, L. E.; Francl, M M. Atomic Charges Derived from Electrostatic Potentials: A Detailed Study. *J. Comput. Chem.* **1987**, *8*, 894−905.
(39) Wold, S.; Ruhe, A.; Wold, H.; Dunn, W. J. The Covariance Problem in Linear Regression. The Partial Least Squares (PLS) Approach to Generalized Inverses. *SIAM J. Sci. Stat. Comput.* **1994**, *5* (3), 735−743.
(40) Cramer, R. D.; Bunce, J. D.; Patterson, D. E.; Frank, I. E. Crossvalidation, Bootstrapping, and Partial Least Squares Compared with Multiple Regression in Conventional QSAR Studies. *Quant. Struct.-Act. Relat.* **1988**, *7*, 18−25.
(41) Waller, C. L.; Oprea, T. I.; Giolitti, A.; Marshall, G. R. Three-Dimensional QSAR of Human Immunodeficiency Virus (I) Protease Inhibitors. 1. A CoMFA Study Employing Experimentally-Determined Alignment Rules. *J. Med. Chem.* **1993**, *36*, 4152−4160.
(42) Cheng, Y. C.; Prusoff, W. H. Relationship between the inhibition constant ($K_i$) and the concentration of inhibitor which causes 50% inhibition ($IC_{50}$) of an enzyme reaction. *Biochem. Pharmacol.* **1973**, *22*, 3099−3108.
(43) Miyashita, M.; Yoshikoshi, A.; Grieco, P. A. Pyridinium *p*-Toluenesulfonate. A Mild and Efficient Catalyst for the Tetrahydropyranylation of Alcohols. *J. Org. Chem.* **1977**, *42*, 3772−3774.
(44) Wallace, O. B.; Springer, D. M. Mild, Selective Deprotection of Thioacetates Using Sodium Thiomethoxide. *Tetrahedron Lett.* **1998**, *39*, 2693−2694.
(45) Teshima, T.; Matsumoto, T.; Wakamiya, T.; Shiba, T.; Aramaki, Y.; Nakajima, T.; Kawai, N. Total Synthesis of NSTX-3, Spider Toxin of *Nephila Maculata*. *Tetrahedron* **1991**, *47*, 3305−3312.
(46) Adams, L. L.; Luzzio, F. A. Ultrasound in Oxochromium (VI)-Amine-Mediated Oxidations-Modifications of the Corey-Suggs Oxidation for the Facile Conversion of Alcohols to Carbonyl Compounds. *J. Org. Chem.* **1989**, *54*, 5387−5390.
(47) Catch, J. R.; Cook, A. H.; Graham, A. R.; Heilbron, I. Synthese of Some Amino acids, Including Methionine. *J. Chem. Soc.* **1947**, 1609−1613.
(48) Corey, E. J.; Suggs, J. W. Pyridinium Chlorochromate. An Efficient Reagent for Oxidation of Primary and Secondary Alcohols to Carbonyl Compounds. *Tetrahedron Lett.* **1975**, 2647−2650.
(49) Easton, N. R.; Cassady, D. R.; Dillard, R. D. Acylation of Ketones in Dimethyl Sulfoxide. *J. Org. Chem.* **1962**, *27*, 2742−2746.
(50) Daeniker, H. U.; Druey, J. Synthese und Eigenschaften von Sulfonsäure-Analoga der d-Amino-lävulinsäure. *Helv. Chim. Acta* **1957**, *40*, 2148−2156.
(51) Fuji, K.; Ichikawa, K.; Node, M.; Fujita, E. Hard Acid and Soft Nucleophile System. New Efficient Method for Removal of Benzyl Protecting Group. *J. Org. Chem.* **1979**, *44*, 1661−1664.

JM980550W